Modelling phytoplankton-virus interactions: phytoplankton blooms and lytic virus transmission

Jimin Zhang[1] · Yawen Yan[1] · Junping Shi[2]

Abstract

A dynamic reaction–diffusion model of four variables is proposed to describe the spread of lytic viruses among phytoplankton in a poorly mixed aquatic environment. The basic ecological reproductive index for phytoplankton invasion and the basic reproduction number for virus transmission are derived to characterize the phytoplankton growth and virus transmission dynamics. The theoretical and numerical results from the model show that the spread of lytic viruses effectively controls phytoplankton blooms. This validates the observations and experimental results of Emiliana huxleyi-lytic virus interactions. The studies also indicate that the lytic virus transmission cannot occur in a low-light or oligotrophic aquatic environment.

1 Introduction

Phytoplankton are the world's most important aquatic producers. They play an essential role in biogeochemical cycles and strongly influence the abundance and biodiversity of aquatic communities. Light and nutrients are two essential resources for phytoplankton growth (Huisman et al. 2006; Klausmeier and Litchman 2001; Wang et al. 2007; Yoshiyama et al. 2009; Zhang et al. 2021). Phytoplankton absorb light

✉ Junping Shi
jxshix@wm.edu

1 School of Mathematical Sciences, Heilongjiang University, Harbin 150080, Heilongjiang, People's Republic of China

2 Department of Mathematics, William & Mary, Williamsburg, VA 23187-8795, USA

energy to synthesize carbon dioxide and water into organic matter and release oxygen (Chen et al. 2015; Davies and Wang 2021). At the same time, they ingest various nutrients from the surrounding environment to preserve normal physiological metabolism (Vasconcelos et al. 2016; Zhang et al. 2018, 2021). These processes are important for achieving energy conversion and elemental cycles in nature and maintaining the carbon-oxygen balance of the atmosphere.

Viruses in aquatic ecosystems are generally small particles. The components of viruses are mainly nucleic acids and protein coats (Fuhrman 1999). This means that viruses can trigger the biosynthesis of the viral genome and protein only when they are parasitic in the host cells (Beretta and Kuang 1998; Edwards and Steward 2018; Fuhrman 1999; Fuhrman et al. 2011). Viruses are extremely abundant and widely distributed over oceans, lakes, and rivers (Suttle 2005). It is shown that viruses are the major pathogens and important causes of mortality for most aquatic organisms (Demory et al. 2021; Fuhrman 1999). As a result, viruses directly affect the structure and stability of aquatic communities.

It is recognized that viruses infect a significant proportion of phytoplankton and it is a major cause of the loss of phytoplankton (Demory et al. 2021; Kuhlisch et al. 2021; Suttle et al. 1990). According to the mechanism of virus transmission among phytoplankton, lytic viruses are considered to be one of the most common viruses (Beretta and Kuang 1998; Edwards and Steward 2018; Fuhrman 1999). The process of the lytic virus infection can be divided into the following steps. First, the virus contacts and adsorbs on phytoplankton cells by random diffusion, and then injects its nucleic acid into the cells. Second, the virus takes over the synthesis machinery of phytoplankton cells and produces viral genome and protein biosynthesis, which is needed for the viral offspring. Third, after the new virus is assembled, the lytic process ends with the lysis of the phytoplankton cell membrane, and then the virus particles are released into aquatic environments. This infection process indicates that lytic viruses destroy phytoplankton cells and reduce the biomass of phytoplankton. In view of the interrelationship between phytoplankton and lytic viruses, it is of great interest to explore the spread of lytic viruses among phytoplankton.

In this study, we propose a mathematical model to describe the spread of lytic viruses among phytoplankton. Here the aquatic environment under consideration is a poorly mixed water column. This suggests that both phytoplankton and virus distributions are spatially heterogeneous (Huisman et al. 2006; Klausmeier and Litchman 2001). Light comes from the water surface and nutrients come from the bottom of the water column (Ryabov et al. 2010; Yoshiyama et al. 2009; Zhang et al. 2021). Phytoplankton growth requires light and nutrients. Lytic viruses move randomly with turbulence and use phytoplankton cells as hosts to replicate and reproduce, eventually releasing a large number of lytic viruses when the cells rupture (Demory et al. 2021; Edwards and Steward 2018; Fuhrman 1999; Kuhlisch et al. 2021). One principal objective of the present paper is to model and elucidate the mechanism of lytic virus transmission among phytoplankton in a heterogeneous environment.

Several mathematical models have been introduced to investigate lytic virus transmission (Béchette et al. 2013; Beretta and Kuang 1998; Demory et al. 2021; Edwards and Steward 2018; Fuhrman et al. 2011). In these existing studies, the basic assumptions are that both phytoplankton and viruses are spatially uniformly distributed.

However, there is growing evidence that only shallow aquatic environments and epilimnion are well-mixed, while most aquatic ecosystems are poorly mixed. This means that phytoplankton generally exhibit strong spatial heterogeneity (Huisman et al. 2006; Klausmeier and Litchman 2001; Ryabov et al. 2010; Yoshiyama et al. 2009; Zhang et al. 2021). Our model consists of four dynamic reaction–diffusion equations. Its contribution is the ability to describe the spatially heterogeneous distribution of phytoplankton and viruses. This model also incorporates the effects of light and phytoplankton sinking relative to existing models of lytic viruses. Thus the reaction–diffusion model contains advection terms and a nonlocal structure. This increases the complexity of the model structure and the difficulty of model analysis. We will rigorously derive the basic ecological reproductive index for phytoplankton invasion and the basic reproduction numbers for lytic virus transmission by analyzing nonnegative steady states and some basic properties of solutions of the model.

Phytoplankton blooms are an important phenomenon in which phytoplankton biomass increases rapidly and significantly over a period of time (Chen et al. 2015; Kuhlisch et al. 2021). It has adverse effects on aquatic ecological environments. Phytoplankton blooms lead to poor water quality of aquatic resources, cause the death of aquatic organisms, and even threaten the health and safety of humans (Ho et al. 2019). It has become apparent that lytic viruses can influence phytoplankton biomass abundance from observations and some experiments (Demory et al. 2021; Edwards and Steward 2018; Fuhrman et al. 2011; Kuhlisch et al. 2021; Suttle et al. 1990). For example, *Emiliana huxleyi* is distributed worldwide and frequently forms large and dense blooms. These blooms are often terminated by the lytic virus transmission (Kuhlisch et al. 2021). Experiments have shown that about 50% of *Emiliana huxleyi* cells are infected by a large double-stranded DNA virus during blooms, and 25–100% *Emiliana huxleyi* deaths are related to the lytic virus infection (Fuhrman 1999; Kuhlisch et al. 2021). Another objective of this study is to examine these observations and experimental results theoretically and reveal the evolution trend in phytoplankton biomass and free lytic virus density with varying ecological factors based on the mathematical model described above.

The structure of the paper is organized as follows. In the next section, a mathematical model consisting of four reaction–diffusion equations is formulated to describe phytoplankton-virus interactions. By using the principal eigenvalue theory, bifurcation theory, and persistence theory, we analyze some basic properties of dynamic solutions and nonnegative steady states of the model in Sect. 3. Two important basic indices are derived. In Sect. 4, numerical bifurcation and time series diagrams are made to explore the role of lytic virus transmission for phytoplankton blooms, and the changes in phytoplankton biomass and free lytic virus density for varying environmental factors. An overview of the main conclusions and future research questions are presented in the last section.

2 Model formulation

The water depth coordinate is x and the time scale is t. Consider a poorly mixed water column with $x = 0$ at the water surface and $x = x_l$ at the bottom of the water column.
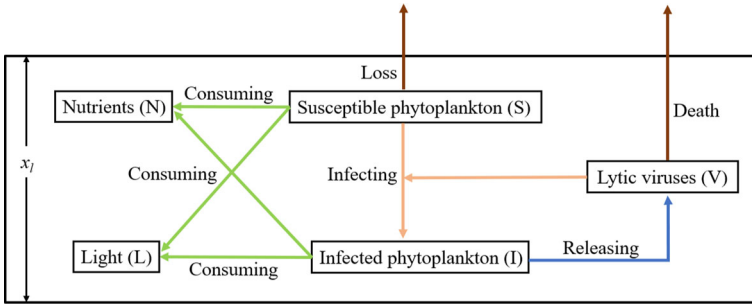
Fig. 1 Phytoplankton-virus interactions in a poorly mixed water column

The model consists of four reaction–diffusion equations describing the change of the concentrations of susceptible phytoplankton ($S(x, t)$), virus-infected phytoplankton ($I(x, t)$), free lytic virus particles ($V(x, t)$), and dissolved nutrients ($N(x, t)$). Their interaction relationship is shown in Fig. 1. The biological significance of variables and parameters in the model is summarized in Table 1.

According to the research work in Beretta and Kuang (1998); Edwards and Steward (2018); Fuhrman et al. (2011), we have the following assumptions:

(A₁) Only susceptible phytoplankton can reproduce through photosynthesis and consumption of nutrients;

(A₂) Virus-infected phytoplankton are removed by lysis before reproducing. The latency period is T from the infection to the lysis. The lytic virus reproduces inside phytoplankton cells during this period T;

(A₃) The lysis of virus-infected phytoplankton releases massive amounts of lytic virus particles.

Let $S(x, t)$ and $I(x, t)$ be the biomass density of susceptible phytoplankton and virus-infected phytoplankton, respectively. They have two different forms of movement in the water column. One is random movement in the vertical direction by turbulence with a diffusivity d_p (Huisman et al. 2006; Klausmeier and Litchman 2001; Ryabov et al. 2010; Yoshiyama et al. 2009; Zhang et al. 2021). The other is directional movement including sinking or buoyant due to gravity or seeking more light with a velocity ω (Grover 2017; Klausmeier and Litchman 2001; Ryabov et al. 2010; Yoshiyama et al. 2009). The whole water column is a closed environment for phytoplankton. This means that $S(x, t)$ and $I(x, t)$ satisfy no-flux boundary conditions at endpoints $x = 0$ and $x = x_l$.

Whether virus-infected phytoplankton can consume resources is still a disputed subject (Gourley and Kuang 2004). Here we introduce a parameter $\theta \in [0, 1]$, which represents the proportion of infected phytoplankton capable of resource consumption (Smith and Thieme 2012). By Assumptions (A₁) and (A₂), the growth of susceptible phytoplankton depends on light and nutrients. It is expressed as

$$rg(N)f(L(x, S + \theta I))S = r \cdot \frac{N}{\gamma + N} \cdot \frac{L(x, S + \theta I)}{h + L(x, S + \theta I)} \cdot S.$$

Table 1 Variables and parameters with realistic values and biological significance of model (2.1)

Symbol	Meaning	Values	Units	Source
t	Time	Variables	day	
x	Depth	Variables	m	
S	Biomass density of susceptible phytoplankton	Variables	cells/m^3	
I	Biomass density of virus-infected phytoplankton	Variables	cells/m^3	
V	Density of free lytic viruses	Variables	virions/m^3	
N	Concentration of dissolved nutrients	Variables	mgN/m^3	
d_p	Vertical turbulent diffusivity of phytoplankton	1 (0.05–5)	m^2/day	Grover (2017); Huisman et al. (2006); Jäger et al. (2010); Klausmeier and Litchman (2001); Ryabov et al. (2010); Yoshiyama et al. (2009)
d_v	Vertical turbulent diffusivity of free lytic virus particles	1 (0.05–5)	m^2/day	Grover (2017); Huisman et al. (2006); Jäger et al. (2010); Klausmeier and Litchman (2001); Ryabov et al. (2010); Yoshiyama et al. (2009)
d_n	Vertical turbulent diffusivity of dissolved nutrients	1 (0.05–5)	m^2/day	Grover (2017); Huisman et al. (2006); Jäger et al. (2010); Klausmeier and Litchman (2001); Ryabov et al. (2010); Yoshiyama et al. (2009)
ω	Directional movement velocity of phytoplankton	0.1(−0.2−0.6)	m/day	Grover (2017); Jäger and Diehl (2014); Jäger et al. (2010); Ryabov et al. (2010)
r	Maximum specific production rate of phytoplankton	1	day^{-1}	Edwards and Steward (2018); Jäger and Diehl (2014); Wang et al. (2007)
μ_p	Loss rate of phytoplankton	0.1	day^{-1}	Jäger et al. (2010); Vasconcelos et al. (2016); Wang et al. (2007)
L^0	Light intensity at the water surface	300	μmol(photons)/(m^2 s)	Jäger et al. (2010); Wang et al. (2007)

Table 1 continued

Symbol	Meaning	Values	Units	Source
l_0	Background light attenuation coefficient	0.4(0.1–2.5)	m^{-1}	Jäger et al. (2010); Vasconcelos et al. (2016); Wang et al. (2007)
l	Light attenuation coefficient of phytoplankton	6×10^{-10}	m^2/cell	Ryabov et al. (2010)
θ	Proportion of virus-infected phytoplankton capable of photosynthesis and nutrient consumption	0.5(0–1)	–	Assumption
γ	Half-saturation constant for nutrient-limited production of phytoplankton	3	mgN/m^3	Jäger and Diehl (2014); Vasconcelos et al. (2016)
h	Half-saturation constant for light-limited production of phytoplankton	100	μmol(photons)/(m^{2}s)	Jäger and Diehl (2014)
β	Transmission coefficient between susceptible phytoplankton and lytic viruses	3.6×10^{-3}	m^{3}cell^{-1}day^{-1}	Edwards and Steward (2018)
η	Intraspecific competition coefficient	0.002	m^{3}cell^{-1}day^{-1}	Assumption
δ	Lytic death rate (1/T)	1.2	day^{-1}	Fuhrman et al. (2011)
μ_v	Death rate of free lytic viruses	0.8(0.2–1.7)	day^{-1}	Edwards and Steward (2018)
q	Lytic virus replication factor, known as "burst size"	10(2–30)	virions cell^{-1}	Béchette et al. (2013); Edwards and Steward (2018); Fuhrman et al. (2011)
b	Infected cells per adsorbed virion	1	cells/virion	Edwards and Steward (2018)
c_p	Nutrient content per phytoplankton cell	0.01	mgN/cell	Assumption
N^0	Nutrient input from the bottom of the water column	50(0–500)	mgN/m^3	Jäger and Diehl (2014); Vasconcelos et al. (2016); Wang et al. (2007)
α	Nutrient exchange rate	0.05	m/day	Jäger and Diehl (2014); Vasconcelos et al. (2016); Yoshiyama et al. (2009)
x_l	Depth of the water column	10	m	Assumption

Here the light intensity $L(x, S + \theta I)$ following the Lambert-Beer law (Huisman et al. 2002) is given by

$$L(x, S + \theta I) = L^0 \exp\left(-l_0 x - l \int_0^x (S(z,t) + \theta I(z,t))dz\right), \ x \in (0, x_l)$$

since light is absorbed by water and phytoplankton above the point x. The reduction of susceptible phytoplankton biomass includes three parts: $-\mu_s S$ (death and grazing Jäger et al. 2010; Vasconcelos et al. 2016; Wang et al. 2007; Zhang et al. 2021), $-\eta(S + \theta I)S$ (competition among phytoplankton for other growth resources such as inorganic carbon for photosynthesis Davies and Wang 2021; Hsu et al. 2017; Nie et al. 2016; Zhang et al. 2021), and $-b\beta SV$ (lytic virus infection into virus-infected phytoplankton (Beretta and Kuang 1998; Edwards and Steward 2018; Fuhrman et al. 2011)). The increase in virus-infected phytoplankton biomass comes from $b\beta SV$ and the loss is owing to the lysis with the lytic death rate $-\delta V$ where $\delta = 1/T$ and T is the latency period from the infection to the lysis.

Let $V(x, t)$ denote the density of free lytic viruses in the water column. By Assumption (A$_3$), its increase is from the lysis release of infected phytoplankton with the lytic virus replication factor q, also known as "burst size" (Beretta and Kuang 1998; Edwards and Steward 2018; Fuhrman et al. 2011). The reduction in V is caused by death with a rate $-\mu_v V$ and infectious consumption with a rate $-\beta SV$. The free lytic virus particles move randomly in the water column under the influence of turbulence with a diffusion rate d_v. Neumann boundary conditions at $x = 0$ and $x = x_l$ mean that no free lytic virus particles enter or leave the water column.

The function $N(x, t)$ describes dissolved nutrient concentration in the water column. The nutrient supply is through the nutrient exchange at the bottom of the water column ($x = x_l$) with a fixed nutrient input concentration N^0 and an exchange rate α (Klausmeier and Litchman 2001; Ryabov et al. 2010; Yoshiyama et al. 2009; Zhang et al. 2018). The nutrients are transported by turbulence in the water column with a diffusion rate d_n. A no-flux boundary condition is imposed at $x = 0$ since there is no nutrient exchange at the water surface. The nutrient consumption in the water column by susceptible and virus-infected phytoplankton is described by a rate $-c_p r g(N) f(L(x, S + \theta I))(S + \theta I)$.

The above assumptions and analysis yield the following complete model for phytoplankton-virus interactions with light and nutrients

$$
\begin{aligned}
S_t &= \underbrace{d_p S_{xx} - \omega S_x}_{\text{diffusion and advection}} + \underbrace{r g(N) f(L(x, S + \theta I))S}_{\text{susceptible phytoplankton growth}} - \underbrace{\mu_p S - \eta(S + \theta I)S}_{\text{susceptible phytoplankton loss}} - \underbrace{b\beta SV}_{\text{infection}}, \\
I_t &= \underbrace{d_p I_{xx} - \omega I_x}_{\text{diffusion and advection}} + \underbrace{b\beta SV}_{\text{infection}} - \underbrace{\delta I}_{\text{lysis death of virus-infected phytoplankton}}, \\
V_t &= \underbrace{d_v V_{xx}}_{\text{diffusion}} + \underbrace{q\delta I}_{\text{lysis release of virus-infected phytoplankton}} - \underbrace{\mu_v V}_{\text{free lytic virus death}} - \underbrace{\beta SV}_{\text{infection}}, \\
N_t &= \underbrace{d_n N_{xx}}_{\text{diffusion}} - \underbrace{c_p r g(N) f(L(x, S + \theta I))(S + \theta I)}_{\text{phytoplankton consumption}},
\end{aligned}
\tag{2.1}
$$

for $x \in (0, x_l)$ and $t > 0$ with the boundary conditions

$$
\begin{aligned}
&d_p S_x(0, t) - \omega S(0, t) = d_p S_x(x_l, t) - \omega S(x_l, t) = 0, \ t > 0, \\
&d_p I_x(0, t) - \omega I(0, t) = d_p I_x(x_l, t) - \omega I(x_l, t) = 0, \ t > 0, \\
&V_x(0, t) = V_x(x_l, t) = 0, \ t > 0, \\
&N_x(0, t) = 0, \ d_n N_x(x_l, t) = \alpha(N^0 - N(x_l, t)) \ (\text{nutrient exchange}), \ t > 0
\end{aligned}
\tag{2.2}
$$

and the initial conditions

$$
\begin{aligned}
&S(x, 0) = S_0(x) \geq \not\equiv 0, \ I(x, 0) = I_0(x) \geq \not\equiv 0, \ x \in (0, x_l), \\
&V(x, 0) = V_0(x) \geq \not\equiv 0, \ N(x, 0) = N_0(x) \geq \not\equiv 0, \ x \in (0, x_l).
\end{aligned}
\tag{2.3}
$$

Here $\omega \in \mathbb{R}, \theta \in [0, 1]$, and remaining parameters are assumed to be positive constants.

Model (2.1) is a system of four reaction–diffusion–advection equations with a nonlocal structure. To explore the phytoplankton-virus interactions, we rigorously analyze the dynamic properties of model (2.1) including basic properties and behavior of solutions and existence and stability of nonnegative steady states.

3 Model analysis

The main purpose of this section is to explore the theoretical results of model (2.1)–(2.3). Some basic properties of solutions of model (2.1)–(2.3) are given in Sect. 3.1. The study of nonnegative steady state solutions is in Sect. 3.2. The dynamic numerical simulations are performed to explain and supplement our theoretical results in Sect. 3.3.

3.1 Basic properties of solutions

Let $X = C([0, x_l], \mathbb{R}^4)$ denote the Banach space of all continuous functions defined on $[0, x_l]$ with values in $\mathbb{R}^4$ and the norm being the supremum norm. The feasible domain $\mathcal{W}$ for (2.1)–(2.3) is the positive cone in X:

$$
\mathcal{W} := \{(S, I, V, N) \in C([0, x_l], \mathbb{R}^4) : S(\cdot) \geq 0, I(\cdot) \geq 0, V(\cdot) \geq 0, N(\cdot) \geq 0\}.
\tag{3.1}
$$

Theorem 3.1 *The system* (2.1)–(2.3) *possesses a unique classical solution in $\mathcal{W}$ for all $t > 0$ and it is dissipative.*

Proof The local existence and uniqueness of nonnegative classical solutions of system (2.1)–(2.3) follow from standard arguments (see Martin and Smith 1990). To obtain the global existence of the solutions, we only need to prove that the solutions of system (2.1)–(2.3) are dissipative.

From the N-equation in (2.1), we obtain

$$N_t \leq d_n N_{xx}, \ x \in (0, x_l), \ t > 0, \ N_x(0, t) = 0,$$
$$d_n N_x(x_l, t) = \alpha(N^0 - N(x_l, t)), \ t > 0.$$

This implies that

$$\limsup_{t \to \infty} N(x, t) \leq N^0 \text{ on } [0, x_l]. \tag{3.2}$$

Let $\hat{S} = Se^{-(\omega/d_p)x}$. From the S-equation, we have

$$\hat{S}_t \leq d_p \hat{S}_{xx} + \omega \hat{S}_x + rf(L^0)\hat{S} - \eta \hat{S}^2 e^{(\omega/d_p)x}, \ x \in (0, x_l), \ t > 0,$$
$$\hat{S}_x(0, t) = \hat{S}_x(x_l, t) = 0, \ t > 0.$$

If $\omega > 0$, then

$$\limsup_{t \to \infty} S(x, t) = \limsup_{t \to \infty} \hat{S}(x, t)e^{(\omega/d_p)x} \leq \frac{rf(L^0)e^{(\omega/d_p)x_l}}{\eta} \text{ on } [0, x_l].$$

If $\omega < 0$, then

$$\limsup_{t \to \infty} S(x, t) = \limsup_{t \to \infty} \hat{S}(x, t)e^{(\omega/d_p)x} \leq \frac{rf(L^0)e^{(-\omega/d_p)x_l}}{\eta} \text{ on } [0, x_l].$$

Hence

$$\limsup_{t \to \infty} S(x, t) \leq \frac{rf(L^0)e^{(|\omega|/d_p)x_l}}{\eta} \text{ on } [0, x_l]. \tag{3.3}$$

From (3.3), for any $\epsilon > 0$, there exists a $t_1 > 0$ such that $S(x, t) \leq rf(L^0)e^{(|\omega|/d_p)x_l}/\eta + \epsilon$ on $[0, x_l]$ for any $t \geq t_1$. Let $\hat{I} = Ie^{-(\omega/d_p)x}$. Adding the S-equation and the I-equation gives

$$(\hat{S} + \hat{I})_t \leq d_p(\hat{S} + \hat{I})_{xx} + \omega(\hat{S} + \hat{I})_x + rf(L^0)\left(\frac{rf(L^0)e^{(|\omega|/d_p)x_l}}{\eta} + \epsilon\right)e^{-(\omega/d_p)x}$$
$$- \min\{\mu_p, \delta\}(\hat{S} + \hat{I})$$

for $x \in (0, x_l)$ and $t > t_1$ with the boundary condition

$$(\hat{S} + \hat{I})_x(0, t) = (\hat{S} + \hat{I})_x(x_l, t) = 0, \ t > t_1.$$

Applying the parabolic comparison theorem, we get

$$\limsup_{t\to\infty} I(x,t) \le \limsup_{t\to\infty} (S+I)(x,t) = \limsup_{t\to\infty} (\hat{S}+\hat{I})e^{(\omega/d_p)x}$$

$$\le \frac{\left(rf(L^0)\right)^2 e^{2(|\omega|/d_p)x_l}}{\eta \min\{\mu_p, \delta\}} \quad \text{on } [0, x_l]. \tag{3.4}$$

For the $\epsilon > 0$ above, there exists a $t_2 > 0$ such that

$$I(x,t) \le \frac{\left(rf(L^0)\right)^2 e^{2(|\omega|/d_p)x_l}}{\eta \min\{\mu_p, \delta\}} + \epsilon \quad \text{on } [0, x_l]$$

for any $t \ge t_2$. From the V-equation in (2.1), we have

$$V_t \le d_v V_{xx} + q\delta \left(\frac{\left(rf(L^0)\right)^2 e^{2(|\omega|/d_p)x_l}}{\eta \min\{\mu_p, \delta\}} + \epsilon\right) - \mu_v V, \ x \in (0, x_l), \ t > t_2,$$

$$V_x(0,t) = V_x(x_l, t) = 0, \ t > t_2.$$

Hence,

$$\limsup_{t\to\infty} V(x,t) \le \frac{q\delta \left(rf(L^0)\right)^2 e^{2(|\omega|/d_p)x_l}}{\eta \mu_v \min\{\mu_p, \delta\}} \quad \text{on } [0, x_l]. \tag{3.5}$$

Combining (3.2)–(3.5) shows that the solutions of system (2.1)–(2.3) are dissipative. This completes the proof.   □

Remark 3.2 By Theorem 3.1, there exists a semiflow $\Theta(t) : \mathcal{W} \to \mathcal{W}$ for (2.1)–(2.3) satisfying

$$\Theta(t)(\sigma_0)(x) = (S(x,t,\sigma_0), I(x,t,\sigma_0), V(x,t,\sigma_0), N(x,t,\sigma_0)), \ x \in [0, x_l], \ t \ge 0$$

for every $\sigma_0 = (S_0, I_0, V_0, N_0) \in \mathcal{W}$. It follows from the dissipativeness of the solutions for (2.1)–(2.3) that $\Theta(t)$ is point dissipative. Furthermore, there exists a global compact attractor for (2.1)–(2.3) in $\mathcal{W}$ from Theorem 3.4.8 in Hale (1988) since $\Theta(t)$ is compact.

3.2 Steady states

In order to investigate the spread of lytic viruses among phytoplankton, we explore nonnegative steady states of model (2.1)–(2.3). There are three types of steady state solutions of model (2.1)–(2.3) as follows.

(i) Extinction steady state $E_1 = (0, 0, 0, N^0)$.

(ii) Disease-free steady state $E_2 = (S_2(x), 0, 0, N_2(x))$, where $S_2(x)$ and $N_2(x)$ satisfy

$$
\begin{aligned}
&d_p S'' - \omega S' + rg(N)f(L(\cdot, S))S - \mu_p S - \eta S^2 = 0, \ x \in (0, x_l), \\
&d_n N'' - c_p rg(N)f(L(\cdot, S))S = 0, \ x \in (0, x_l), \\
&d_p S'(0) - \omega S(0) = d_p S'(x_l) - \omega S(x_l) = 0, \\
&N'(0) = 0, \ d_n N'(x_l) = \alpha(N^0 - N(x_l)).
\end{aligned}
\tag{3.6}
$$

(iii) Endemic steady state $E_3 = (S_3(x), I_3(x), V_3(x), N_3(x))$, where $S_3(x)$, $I_3(x)$, $V_3(x)$ and $N_3(x)$ satisfy

$$
\begin{aligned}
&d_p S'' - \omega S' + rg(N)f(L(\cdot, S + \theta I))S - \mu_p S - \eta(S + \theta I)S - b\beta SV = 0, \\
&d_p I'' - \omega I' + b\beta SV - \delta I = 0, \\
&d_v V'' + q\delta I - \mu_v V - \beta SV = 0, \\
&d_n N'' - c_p rg(N)f(L(\cdot, S + \theta I))(S + \theta I) = 0
\end{aligned}
\tag{3.7}
$$

on $(0, x_l)$ with the boundary conditions

$$
\begin{aligned}
&d_p S'(0) - \omega S(0) = d_p S'(x_l) - \omega S(x_l) = 0, \\
&d_p I'(0) - \omega I(0) = d_p I'(x_l) - \omega I(x_l) = 0, \\
&V'(0) = V'(x_l) = 0, \ N'(0) = 0, \ d_n N'(x_l) = \alpha(N^0 - N(x_l)).
\end{aligned}
\tag{3.8}
$$

To characterize the dynamic behavior of model (2.1)–(2.3), we define the basic ecological reproductive index for phytoplankton invasion. For $h \in L^\infty([0, x_l])$, let $\lambda_1(d_p, \omega, x_l, h(x))$ denote the principal eigenvalue of

$$
\begin{aligned}
&d_p \phi''(x) - \omega \phi'(x) + h(x)\phi(x) = \lambda \phi(x), \ x \in (0, x_l), \\
&d_p \phi'(0) - \omega \phi(0) = d_p \phi'(x_l) - \omega \phi(x_l) = 0.
\end{aligned}
\tag{3.9}
$$

By Proposition 3.1 in Wang et al. (2019), λ_1 exists and it is unique. Moreover, $\lambda_1(d_p, \omega, x_l, h_1(x)) \geq \lambda_1(d_p, \omega, x_l, h_2(x))$ if $h_1(x) \geq h_2(x)$ on $[0, x_l]$. The basic ecological reproductive index for phytoplankton invasion is defined as

$$
R_p = \frac{\mu_p^*}{\mu_p}, \quad \text{where} \quad \mu_p^* = \lambda_1(d_p, \omega, x_l, rg(N^0)f(L(x, 0))).
\tag{3.10}
$$

Note that μ_p^* is related to the stability of the unique extinction steady state E_1 (see (3.11)). The index R_p measures the reproductive capacity of phytoplankton, and it describes the average number of new phytoplankton cells produced by per cubic meter of phytoplankton in a life cycle.

Theorem 3.3 $E_1 \equiv (0, 0, 0, N^0)$ *is the unique extinction steady state of* (2.1)–(2.3). *If $R_p < 1$, then E_1 is globally asymptotically stable, while E_1 is unstable if $R_p > 1$.*

Proof It is clear that $E_1 \equiv (0, 0, 0, N^0)$ exists uniquely. The local stability of E_1 is determined by the eigenvalue problem

$$
\begin{aligned}
\lambda\xi &= d_p\xi''(x) - \omega\xi'(x) + \left(rg(N^0)f(L(x,0)) - \mu_p\right)\xi, \ x \in (0, x_l), \\
\lambda\varphi &= d_p\varphi''(x) - \omega\varphi'(x) - \delta\varphi, \ x \in (0, x_l), \\
\lambda\psi &= d_v\psi''(x) + q\delta\varphi - \mu_v\psi, \ x \in (0, x_l), \\
\lambda\zeta &= d_n\zeta''(x) - c_p rg(N^0)f(L(x,0))(\xi + \theta\varphi), \ x \in (0, x_l)
\end{aligned}
\tag{3.11}
$$

with the boundary conditions

$$d_p\xi'(0) - \omega\xi(0) = d_p\xi'(x_l) - \omega\xi(x_l) = 0, \tag{3.12a}$$
$$d_p\varphi'(0) - \omega\varphi(0) = d_p\varphi'(x_l) - \omega\varphi(x_l) = 0, \tag{3.12b}$$
$$\psi'(0) = \psi'(x_l) = 0, \tag{3.12c}$$
$$\zeta'(0) = 0, \ d_n\zeta'(x_l) = -\alpha\zeta(x_l). \tag{3.12d}$$

One can observe that λ is an eigenvalue of (3.11) if and only if λ is an eigenvalue of one of the following four operators

$$
d_p\frac{d^2}{dx^2} - \omega\frac{d}{dx} + \left(rg(N^0)f(L(\cdot, 0)) - \mu_p\right),
$$
$$
d_p\frac{d^2}{dx^2} - \omega\frac{d}{dx} - \delta, \ d_v\frac{d^2}{dx^2} - \mu_v, \ d_n\frac{d^2}{dx^2}
$$

with the boundary conditions (3.12a)–(3.12d) (see Theorem 4.1 in Nie et al. 2017). Note that all eigenvalues of the operators $d_v\frac{d^2}{dx^2} - \mu_v$ with the Neumann boundary condition (3.12c) and $d_n\frac{d^2}{dx^2}$ with the Robin boundary condition (3.12d) are less than 0. By (3.9), all eigenvalues of the operator $d_p\frac{d^2}{dx^2} - \omega\frac{d}{dx} - \delta$ with (3.12b) are less than 0. Applying (3.9) again, all eigenvalues of the operator $d_p\frac{d^2}{dx^2} - \omega\frac{d}{dx} + \left(rg(N^0)f(L(\cdot, 0)) - \mu_p\right)$ with (3.12a) are less than 0 if $R_p < 1$, and it has at least one eigenvalue greater than 0 if $R_p > 1$. The above analysis shows that E_1 is locally asymptotically stable when $R_p < 1$, and E_1 is unstable when $R_p > 1$.

To obtain the global stability of E_1 when $R_p < 1$, we only need to prove that it is globally attractive. For any $\epsilon > 0$, from (3.2) and (3.5), there exists a $t_1^* > 0$ such that $N(\cdot, t) \le N^0 + \epsilon$ and $V(\cdot, t) \le q\delta\left(rf(L^0)\right)^2 e^{2(|\omega|/d_p)x_l}/(\eta\mu_v \min\{\mu_p, \delta\}) + \epsilon$ for $t \ge t_1^*$. Let ξ be the first component of the positive eigenfunction of (3.11) corresponding to $\mu = \mu_p^*$ satisfying $S(x, t_1^*) \le c\xi(x)$ for some $c > 0$. Let $\hat{S} = Se^{-(\omega/d_p)x}$ and $\hat{\xi} = \xi e^{-(\omega/d_p)x}$. It follows from the S-equation in model (2.1) that

$$
\hat{S}_t \le d_p\hat{S}_{xx} + \omega\hat{S}_x + rg(N^0 + \epsilon)f(L(x, 0))\hat{S} - \mu_p\hat{S}, \ x \in (0, x_l), \ t > t_1^*,
$$

$$\hat{S}_x(0, t) = \hat{S}_x(x_l, t) = 0, \ t > t_1^*.$$

By the comparison theorem of parabolic systems, we have

$$\hat{S}(x, t) \leq ce^{-(\mu_p - \lambda_1(d_p, \omega, x_l, rg(N^0 + \epsilon)f(L(x,0))))(t - t_1^*)}\hat{\xi}(x), \ x \in [0, x_l], \text{ for any } t \geq t_1^*.$$

This shows that $\limsup_{t\to\infty} S(x, t) = \limsup_{t\to\infty} \hat{S}(x, t)e^{(\omega/d_p)x} = 0$ on $[0, x_l]$ since $R_p < 1$ and ϵ is sufficiently small. Hence we can find a $t_2^* > t_1^*$ satisfying $S(x, t) \leq \epsilon$ on $[0, x_l]$ for any $t \geq t_2^*$. Let $\hat{I} = Ie^{-(\omega/d_p)x}$. It follows that

$$\hat{I}_t \leq d_p\hat{I}_{xx} + \omega\hat{I}_x + b\beta\epsilon \left(\frac{q\delta \left(rf(L^0)\right)^2 e^{2(|\omega|/d_p)x_l}}{\eta\mu_v \min\{\mu_p, \delta\}} + \epsilon \right)$$

$$e^{-(\omega/d_p)x} - \delta\hat{I}, \ x \in (0, x_l), \ t > t_2^*,$$

$$\hat{I}_x(0, t) = \hat{I}_x(x_l, t) = 0, \ t > t_2^*.$$

Then

$$\limsup_{t\to\infty} I(x, t) = \limsup_{t\to\infty} \hat{I}(x, t)e^{(\omega/d_p)x} = 0 \text{ on } [0, x_l] \qquad (3.13)$$

since ϵ is sufficiently small. Similarly, we can also obtain

$$\limsup_{t\to\infty} V(x, t) = 0 \text{ on } [0, x_l]. \qquad (3.14)$$

Following Theorem 1.8 in Mischaikow et al. (1995) or Theorem 4.1 in Thieme (1992), the N-equation in (2.1) becomes

$$N_t = d_n N_{xx}, \ x \in (0, x_l), \ N_x(0, t) = 0, \ d_n N_x(x_l, t) = \alpha(N^0 - N(x_l, t))$$

for sufficiently large t. Thus

$$\lim_{t\to\infty} N(x, t) = N^0 \text{ on } [0, x_l], \qquad (3.15)$$

and then E_1 is globally attractive. $\qquad\qquad\qquad\qquad\qquad\qquad\qquad\qquad \square$

Remark 3.4 1. The basic ecological reproductive index for phytoplankton invasion R_p measures the viability of phytoplankton. $R_p < 1$ means that phytoplankton go extinct and nutrients are evenly distributed in the water column. $\mu_p = \mu_p^*$ is a critical loss rate that determines whether phytoplankton can invade an aquatic ecosystem.

2. From the structure of (3.10), the basic ecological reproductive index R_p depends on important ecological parameters such as spatial factors d_p, ω, the water column depth x_l, nutrient concentration at the bottom of the water column N^0 and light intensity at the water surface L^0. According to Theorems 3.2 and 3.4 in Hsu and Lou

(2010), we conclude that $dR_p/d\omega < 0$ and $dR_p/dx_l < 0$. By the monotonicity of λ_1 with respect to $rg(N^0)f(L(x,0))$, $dR_p/dN^0 > 0$ and $dR_p/dL^0 > 0$. Thus, high N^0 and L^0 are conducive to phytoplankton invasion, while high ω and x_l prevent phytoplankton invasion. The dependence of R_p on d_p is complicated. Both high and low d_p may be detrimental to the survival of phytoplankton (see Huisman et al. 2002).

When $R_p > 1$, the extinction state E_1 is unstable and phytoplankton can persist. To establish the existence of E_2 which has a positive phytoplankton mass, we first derive *a priori* estimate for nonnegative solutions of (3.6).

Lemma 3.5 *Suppose $(S_2(x), N_2(x))$ is a nonnegative solution of (3.6) with $S_2, N_2 \not\equiv 0$. Then $0 < N_2(x) < N^0, 0 < S_2(x) \leq ((rg(N^0)f(L^0)+\mu_p)e^{(|\omega|/d_p)x_l})/\eta$ on $[0, x_l]$ and $0 < \mu_p < \mu_p^*$.*

Proof Let $\bar{U}(x) = e^{-(\omega/d_p)x} S_2(x)$. Then $\bar{U}$ satisfies

$$-d_p\bar{U}'' - \omega\bar{U}' + \left(\mu_p + \eta\bar{U}e^{(\omega/d_p)x}\right)\bar{U} = rg(N_2)f(L(x, S_2))\bar{U} \geq 0, \ x \in (0, x_l),$$

$$\bar{U}'(0) = \bar{U}'(x_l) = 0.$$

From the strong maximum principle and Hopf boundary lemma, we have $S_2(x) = \bar{U}(x)e^{(\omega/d_p)x} > 0$ on $[0, x_l]$. It follows from (3.6) that

$$\alpha(N^0 - N_2(x_l)) = \int_0^{x_l} c_p rg(N_2(x))f(L(x, S_2(x)))S_2(x)dx$$

$$= c_p \int_0^{x_l} \left(\mu_p S_2(x) + \eta S_2^2(x)\right) dx > 0,$$

and then $N_2(x_l) < N^0$. By the N-equation in (3.6), we obtain

$$-d_n N_2'' + \left(c_p rf(L(x, S_2))S_2 \int_0^1 g'(sN_2)ds\right) N_2 = 0, \ x \in (0, x_l),$$

$$N_2'(0) = 0, \ d_n N_2'(x_l) = \alpha(N^0 - N_2(x_l)) > 0.$$

This implies that $N_2(x) > 0$ on $[0, x_l]$ from the maximum principle. Note that

$$d_n N_2'' = c_p rg(N_2)f(L(x, S_2))S_2 > 0, \ x \in (0, x_l).$$

Combining its boundary conditions give $N_2'(x) > 0$ on $(0, x_l)$. Thus, $0 < N_2 < N^0$ on $[0, x_l]$.

From the S-equation in (3.6) and $S_2 > 0$, we get

$$\mu_p = \lambda_1(d_p, \omega, x_l, rg(N_2)f(L(x, S_2)) - \eta S_2)$$

$$< \lambda_1(d_p, \omega, x_l, rg(N^0)f(L(x, 0))) = \mu_p^*.$$

By applying the similar arguments of Lemma 2.2 in Pang et al. (2019), we can conclude that $S_2(x) \leq ((rg(N^0)f(L^0) + \mu_p)e^{(|\omega|/d_p)x_l})/\eta$ on $[0, x_l]$. □

We now prove the existence of disease-free steady state E_2 by showing E_2 bifurcating from the line of extinction state $\{(\mu_p, E_1) : \mu_p > 0\}$ at $\mu_p = \mu_p^*$.

Theorem 3.6 (i) *If $R_p > 1$ (equivalently, $\mu_p \in (0, \mu_p^*)$), then (2.1)–(2.3) has at least one disease-free steady state E_2.*

(ii) *There exists an $\varepsilon > 0$ such that for each given $s \in (0, \varepsilon)$ the bifurcating solution $(\mu_p(s), S_2(s, \cdot), N_2(s, \cdot))$ is locally asymptotically stable with respect to the susceptible phytoplankton-nutrient model*

$$
\begin{aligned}
&S_t = d_p S_{xx} - \omega S_x + rg(N)f(L(x, S))S - \mu_p S - \eta S^2, \ x \in (0, x_l), \ t > 0, \\
&N_t = d_n N_{xx} - c_p rg(N)f(L(x, S))S, \ x \in (0, x_l), \ t > 0, \\
&d_p S_x(0, t) - \omega S(0, t) = d_p S_x(x_l, t) - \omega S(x_l, t) = 0, \ t > 0, \\
&N_x(0, t) = 0, \ d_n N_x(x_l, t) = \alpha(N^0 - N(x_l, t)), \ t > 0.
\end{aligned} \tag{3.16}
$$

Proof (i) The first part of the proof is divided into two steps. The first one is to obtain the existence of local bifurcation of E_2. Applying the Crandall–Rabinowitz bifurcation theorem (see Theorem 1.7 in Crandall and Rabinowitz 1971), we show that there is a positive solution branch $\Pi_2^+ = \{(\mu_p(s), S_2(s, \cdot), N_2(s, \cdot)) : 0 < s < \varepsilon\}$ for some $\varepsilon > 0$ from $\Pi_1 = \{(\mu_p, 0, N^0) : \mu_p > 0\}$ at $\mu_p = \mu_p^*$. The second is to explore the global bifurcation structure of E_2. That is to show that the disease-free steady state E_2 exists for all $\mu_p \in (0, \mu_p^*)$ by using Theorem 3.3 and Remark 3.4 in Shi and Wang (2009).

Let $\tilde{S} = Se^{-(\omega/d_p)x}$ and $\tilde{N} = N^0 - N$. Then (3.6) is transformed into

$$
\begin{aligned}
&d_p \tilde{S}'' + \omega \tilde{S}' + rg(N^0 - \tilde{N})f(L(x, \tilde{S}e^{(\omega/d_p)x}))\tilde{S} \\
&\quad - \mu_p \tilde{S} - \eta \tilde{S}^2 e^{(\omega/d_p)x} = 0, \ x \in (0, x_l), \\
&- d_n \tilde{N}'' - c_p rg(N^0 - \tilde{N})f(L(x, \tilde{S}e^{(\omega/d_p)x}))\tilde{S}e^{(\omega/d_p)x} = 0, \ x \in (0, x_l), \\
&\tilde{S}'(0) = \tilde{S}'(x_l) = 0, \ \tilde{N}'(0) = d_n \tilde{N}'(x_l) + \alpha \tilde{N}(x_l) = 0
\end{aligned} \tag{3.17}
$$

and the extinction state $(S, N) = (0, N^0)$ is transformed to $(\tilde{S}, \tilde{N}) = (0, 0)$. Set $\mathbb{W} := \mathbb{W}_1 \times \mathbb{W}_2$, where

$$
\begin{aligned}
\mathbb{W}_1 &:= \{h \in W^{2,p}(0, x_l) : h'(0) = h'(x_l) = 0\}, \\
\mathbb{W}_2 &:= \{h \in W^{2,p}(0, x_l) : h'(0) = d_n h'(x_l) + \alpha h(x_l) = 0\}.
\end{aligned}
$$

Step 1 (Local bifurcation). Define $T : \mathbb{R}^+ \times \mathbb{W} \to L^p(0, x_l) \times L^p(0, x_l)$, $p > 1$ as follows

$$
T(\mu_p, \tilde{S}, \tilde{N}) = \begin{pmatrix} d_p \tilde{S}'' + \omega \tilde{S}' + rg(N^0 - \tilde{N})f(L(x, \tilde{S}e^{(\omega/d_p)x}))\tilde{S} - \mu_p \tilde{S} - \eta \tilde{S}^2 e^{(\omega/d_p)x} \\ -d_n \tilde{N}'' - c_p rg(N^0 - \tilde{N})f(L(x, \tilde{S}e^{(\omega/d_p)x}))\tilde{S}e^{(\omega/d_p)x} \end{pmatrix}.
$$

It can be directly observed that $T(\mu_p, 0, 0) = 0$ for $\mu_p > 0$. Let $Q := T_{(\tilde{S}, \tilde{N})}(\mu_p^*, 0, 0)$. A direct calculation shows that

$$Q[\xi, \zeta] = \begin{pmatrix} d_p\xi'' + \omega\xi' + \left(rg(N^0)f(L(x,0)) - \mu_p^*\right)\xi \\ -d_n\zeta'' - c_prg(N^0)f(L(x,0))\xi e^{(\omega/d_p)x} \end{pmatrix}$$

for any $(\xi, \zeta) \in \mathbb{W}$.

We claim that Q is a Fredholm operator with index zero. Following the proof of Theorem 3.5 in Yan et al. (2022), we have dim ker $Q = 1$ and ker $Q = \text{span}\{(\bar{\xi}, \bar{\zeta})\}$ with $\bar{\xi} > 0, \bar{\zeta} > 0$ on $[0, x_l]$. Here $\bar{\xi} \in \mathbb{W}_1$ satisfies

$$d_p\bar{\xi}'' + \omega\bar{\xi}' + \left(rg(N^0)f(L(x,0)) - \mu_p^*\right)\bar{\xi} = 0, \ x \in (0, x_l), \qquad (3.18)$$

and $\bar{\zeta} \in \mathbb{W}_2$ can be uniquely solved by

$$-d_n\zeta'' - c_prg(N^0)f(L(x,0))\bar{\xi}e^{(\omega/d_p)x} = 0, \ x \in (0, x_l).$$

If $(\kappa_1, \kappa_2) \in \text{range } Q$, then we can find $(\hat{\xi}, \hat{\zeta}) \in \mathbb{W}$ satisfying

$$\begin{aligned} d_p\hat{\xi}'' + \omega\hat{\xi}' + \left(rg(N^0)f(L(x,0)) - \mu_p^*\right)\hat{\xi} &= \kappa_1, \ x \in (0, x_l), \\ -d_n\hat{\zeta}'' - c_prg(N^0)f(L(x,0))\hat{\xi}e^{(\omega/d_p)x} &= \kappa_2, \ x \in (0, x_l). \end{aligned} \qquad (3.19)$$

By (3.18) and the first equation in (3.19), we have $\int_0^{x_l} \kappa_1(x)e^{(\omega/d_p)x}\bar{\xi}(x)dx = 0$, and $\hat{\xi} \in \mathbb{W}_1$ can be uniquely solved under this condition. It follows from the Fredholm alternative theorem that $\hat{\zeta} \in \mathbb{W}_2$ can then be uniquely solved by the second equation in (3.19). Hence,

$$\text{range } Q = \left\{(\kappa_1, \kappa_2) \in L^p(0, x_l) \times L^p(0, x_l) : \int_0^{x_l} \kappa_1(x)e^{(\omega/d_p)x}\bar{\xi}(x)dx = 0\right\}$$

and codim range $Q = 1$. This implies that Q is a Fredholm operator with index zero.

One can observe that $T_{(\mu_p, (\tilde{S}, \tilde{N}))}(\mu_p^*, 0, 0)(\bar{\xi}, \bar{\zeta}) = (-\bar{\xi}, 0, 0)$ and $\int_0^{x_l} e^{(\omega/d_p)x} \bar{\xi}^2(x)dx \neq 0$. Then $T_{(\mu_p, (\tilde{S}, \tilde{N}))}(\mu_p^*, 0, 0) \notin \text{range } Q$. According to the Crandall–Rabinowitz bifurcation theorem (Theorem 1.7 in Crandall and Rabinowitz (1971)), there is a smooth curve $\tilde{\Pi}_2 = \{(\mu_p(s), \tilde{S}(s, \cdot), \tilde{N}(s, \cdot)) : -\varepsilon < s < \varepsilon\}$ for some $\varepsilon > 0$ satisfying (3.17) near $(\mu_p^*, 0, 0)$ with the form

$$\tilde{S}(s, \cdot) = s\bar{\xi}(\cdot) + o(s), \ \tilde{N}(s, \cdot) = s\bar{\zeta}(\cdot) + o(s).$$

Here we also define

$$\tilde{\Pi}_2^+ = \{(\mu_p(s), \tilde{S}(s, \cdot), \tilde{N}(s, \cdot)) : 0 < s < \varepsilon\},$$

$$\tilde{\Pi}_2^- = \{(\mu_p(s), \tilde{S}(s, \cdot), \tilde{N}(s, \cdot)) : -\varepsilon < s < 0\}.$$

Let $S_2(s, x) = \tilde{S}(s, x)e^{(\omega/d_p)x}$, $N_2(s, x) = N^0 - \tilde{N}(s, x)$ on $[0, x_l]$, and define

$$\Pi_2^+ = \{(\mu_p(s), S_2(s, \cdot), N_2(s, \cdot)) : 0 < s < \varepsilon\},$$
$$\Pi_2^- = \{(\mu_p(s), S_2(s, \cdot), N_2(s, \cdot)) : -\varepsilon < s < 0\}.$$

Then the bifurcating branch Π_2^+ consists of positive solutions of (3.6) as $\bar{\xi} > 0$ and $N^0 > 0$.

Let

$$\pi(x, \bar{\xi}, \bar{\zeta}) = -\frac{hlL(x, 0)g(N^0)}{(h + L(x, 0))^2} \int_0^x \bar{\xi}(z)e^{(\omega/d_p)z}dz - \eta\bar{\xi}e^{(\omega/d_p)x} - \frac{\gamma f(L(x, 0))}{(\gamma + N^0)^2}\bar{\zeta}.$$

Then

$$\mu_p'(0) = -\frac{\left\langle \mathcal{L}, T_{((\tilde{S}, \tilde{N})(\tilde{S}, \tilde{N}))}\left(\mu_p^*, 0, 0\right)[\bar{\xi}, \bar{\zeta}]^2 \right\rangle}{2\left\langle \mathcal{L}, T_{(\mu_p, (\tilde{S}, \tilde{N}))}\left(\mu_p^*, 0, 0\right)[\bar{\xi}, \bar{\zeta}]\right\rangle} = \frac{\int_0^{x_l} re^{(\omega/d_p)x}\pi(x, \bar{\xi}, \bar{\zeta})\bar{\xi}^2dx}{\int_0^{x_l} e^{(\omega/d_p)x}\bar{\xi}^2dx} < 0,$$

where $\mathcal{L}$ is a linear functional on $L^p(0, x_l) \times L^p(0, x_l)$ defined by

$$\langle \mathcal{L}, (\kappa_1, \kappa_2) \rangle = \int_0^{x_l} \kappa_1(x)e^{(\omega/d_p)x}\bar{\xi}dx.$$

This shows that the bifurcation of Π_2^+ or $\tilde{\Pi}_2^+$ at $(0, N^0)$ is backward as $\pi < 0$.

Step 2 (Global bifurcation). In view of Theorem 4.3 in Shi and Wang (2009), there exists a connected component $\tilde{\Gamma}$ of $\overline{\Sigma}$ containing $\tilde{\Pi}_2$ where $\Sigma = \{(\mu_p, \tilde{S}, \tilde{N}) \in \mathbb{R}^+ \times \mathbb{W} : T(\mu_p, \tilde{S}, \tilde{N}) = 0, (\tilde{S}, \tilde{N}) \neq (0, 0)\}$. Let $\tilde{\Gamma}^+$ be the connected component of $\tilde{\Gamma}\backslash\tilde{\Pi}_2^-$ which contains $\tilde{\Pi}_2^+$. It follows from Theorem 4.4 in Shi and Wang (2009) that $\tilde{\Gamma}^+$ satisfies one of the following three alternatives: (1) it is not compact in $\mathbb{R}^+ \times \mathbb{W}$, (2) it contains another point $(\bar{\mu}_p, 0, 0)$ with $\bar{\mu}_p \neq \mu_p^*$, (3) it contains a point $(\mu_p, \bar{S}, \bar{N})$ with $0 \neq (\bar{S}, \bar{N}) \in Z$, where Z is a closed complement of $\ker Q = \text{span}\{(\bar{\xi}, \bar{\zeta})\}$.

Assume that (2) occurs. Then $(\bar{\mu}_p, 0, 0)$ is a bifurcation point for $T = 0$ with $\bar{\mu}_p \neq \mu_p^*$ and 0 is an eigenvalue of $T_{(\tilde{S}, \tilde{N})}(\mu_p, 0, 0)$ and $\bar{\mu}_p < \mu_p^*$. There are only finitely many such $\bar{\mu}_p$, so without loss of generality we may assume that Γ^+ does not contain any other $(\mu_p, 0, 0)$ with $\bar{\mu}_p < \mu_p < \mu_p^*$. Since $\mu_p = \mu_p^*$ is the only value such that $T_{(\tilde{S}, \tilde{N})}(\mu_p, 0, 0)$ has a positive eigenfunction corresponding to a zero eigenvalue, then all solutions of $T(\mu_p, \tilde{S}, \tilde{N}) = 0$ on $\tilde{\Gamma}^+$ near $(\bar{\mu}_p, 0, 0)$ must be sign-changing. Since $\tilde{\Gamma}^+ \supseteq \tilde{\Pi}_2^+$, then there exists $(\mu_p, \tilde{S}, \tilde{N}) \in \tilde{\Gamma}^+$ which satisfies $\tilde{S} > 0$ and $\tilde{N} > 0$. From the connectedness of Γ^+, there exists $(\hat{\mu}_p, \tilde{S}, \tilde{N}) \in \tilde{\Gamma}^+$ with $\hat{\mu}_p \in [\bar{\mu}_p, \mu_p^*)$ and $x_0 \in [0, x_l]$ such that either $\tilde{S}(x_0) = 0$ or $\tilde{N}(x_0) = 0$, but $\tilde{S}(x) \geq 0$ and $\tilde{N}(x) \geq 0$ for all $x \in [0, x_l]$. If $\tilde{S}(x_0) = 0$, then we also have $\tilde{S}'(x_0) = 0$, then we obtain $\tilde{S} \equiv \tilde{N} = 0$ on $[0, x_l]$ from the uniqueness of solution to ODE so (2) occurs

at $\hat{\mu}_p$ and $\hat{\mu}_p = \bar{\mu}_p$. But the solution $(\hat{\mu}_p, \tilde{S}, \tilde{N})$ is not sign-changing, which is a contradiction. Hence we must have $\tilde{S}(x) > 0$ on $[0, x_l]$ and $\tilde{N}(x_0) = 0$. But this leads to another contradiction using $\tilde{S} \geq 0$ and maximum principle. Hence (2) cannot occur. Assume that (3) happens. Since $0 \neq (\bar{S}, \bar{N}) \in Z$, then either $\bar{S}$ or $\bar{N}$ is sign-changing as $\bar{\xi} >$ and $\bar{\zeta} > 0$. We can follow the similar proof as in the one for alternative (2) to show (3) cannot occurs.

Hence the alternative (1) must occur and the connected component $\tilde{\Gamma}^+$ is not compact in $\mathbb{R}^+ \times \mathbb{W}$. Moreover the proof in the last paragraph implies that if $(\mu_p, \tilde{S}, \tilde{N}) \in \tilde{\Gamma}^+$ then $\tilde{S} > 0$ and $\tilde{N} > 0$. Let

$$\Gamma^+ = \{(\mu_p, S, N) : S = \tilde{S}e^{(\omega/d_p)x}, N = N^0 - \tilde{N}, \text{ and } (\mu_p, \tilde{S}, \tilde{N}) \in \tilde{\Gamma}^+\}.$$

Then for any $(\mu_p, S, N) \in \Gamma^+$, we know that $S = \tilde{S}e^{(\omega/d_p)x} > 0$ on $[0, x_l]$, then $N > 0$ on $[0, x_l]$ since $N'(0) = 0$ and $N'' > 0$ in $(0, x_l)$. From Lemma 3.5, every positive solution of (3.6) is bounded for $0 < \mu_p < \mu_p^*$ and there is no positive solution of (3.6) for $\mu_p \geq \mu_p^*$. Therefore Γ^+ can be extended to $\mu_p = 0$ and the projection of Γ^+ onto μ_p-axis contains $(0, \mu_p^*)$.

(ii) Let $\mathcal{L}(\mu_p(s), S(s), N(s))$ be the linearized operator of (3.16) at $(\mu_p(s), S(s), N(s))$. From Corollary 1.13 and Theorem 1.16 in Crandall and Rabinowitz (1973), there exist continuously differentiable functions

$$\gamma_1 : [\mu_p^*, \mu_p^* + \varepsilon) \to \mathbb{R}, \ (\xi_1, \zeta_1) : [\mu_p^*, \mu_p^* + \varepsilon) \to W^{2,p}(0, x_l) \times W^{2,p}(0, x_l),$$

$$\gamma_2 : [0, \varepsilon) \to \mathbb{R}, \ (\xi_2, \zeta_2) : [0, \varepsilon) \to W^{2,p}(0, x_l) \times W^{2,p}(0, x_l)$$

such that

$$\mathcal{L}(\mu_p, 0, N^0)[\xi_1(\mu_p), \zeta_1(\mu_p)] = \gamma_1(\mu_p)[\xi_1(\mu_p), \zeta_1(\mu_p)],$$
$$\mathcal{L}(\mu_p(s), S_2(s, \cdot), N_2(s, \cdot))[\xi_2(s), \zeta_2(s)] = \gamma_2(s)[\xi_2(s), \zeta_2(s)]$$

and

$$\lim_{s \to 0^+} \frac{-s\mu_p'(s)\gamma_1'(\mu_p^*)}{\gamma_2(s)} = 1.$$

Here $\gamma_1(\mu_p^*) = \gamma_2(0) = 0$ and $(\xi_1(\mu_p^*), \zeta_1(\mu_p^*)) = (\xi_2(0), \zeta_2(0)) = (\bar{\xi}, \bar{\zeta})$. Note that $\gamma_1(\mu_p)$ is a simple eigenvalue of

$$d_p\xi'' - \omega\xi' + \left(rg(N^0)f(L(x, 0)) - \mu_p\right)\xi = \gamma_1(\mu_p)\xi, \ x \in (0, x_l),$$
$$d_p\xi'(0) - \omega\xi(0) = d_p\xi'(x_l) - \omega\xi(x_l) = 0.$$

It follows that $\gamma_1(\mu_p) = \mu_p^* - \mu_p$ and then $\gamma_1'(\mu_p^*) = -1$. Recalling $\mu_p'(0) < 0$, we have $\gamma_2(s) < 0$ for $s \in (0, \varepsilon)$. By the perturbation theory of linear operators (see [22]), $\gamma_2(s)$ is also the principal eigenvalue of $\mathcal{L}(\mu_p(s), S_2(s, \cdot), N_2(s, \cdot))$ when s is

sufficiently small. This means that $(S_2(s, \cdot), N_2(s, \cdot))$ is locally asymptotically stable for (3.16). □

In Theorem 3.6, we obtain the existence of E_2 for all $0 < \mu_p < \mu_p^*$, and the uniqueness and stability of E_2 is unknown. Numerical simulations suggest that the disease-free steady state E_2 is unique if $R_p > 1$.

Next we show that when $R_p > 1$ and some additional conditions are satisfied, solutions of model (2.1)–(2.3) are uniformly persistent and there exists at least one endemic steady state E_3. To obtain the conclusions, we define the basic reproduction number for lytic virus transmission. Letting $\bar{I} = I e^{-(\omega/d_p)x}$ and linearizing (2.1) at a disease-free steady state $E_2 = (S_2, 0, 0, N_2)$, we obtain

$$
\begin{aligned}
&\bar{I}_t = d_p \bar{I}_{xx} + \omega \bar{I}_x + b\beta e^{-(\omega/d_p)x} S_2 V - \delta \bar{I}, \ x \in (0, x_l), \ t > 0, \\
&V_t = d_v V_{xx} + q\delta e^{(\omega/d_p)x} \bar{I} - \mu_v V - \beta S_2 V, \ x \in (0, x_l), \ t > 0, \\
&\bar{I}_x(0, t) = \bar{I}_x(x_l, t) = V_x(0, t) = V_x(x_l, t) = 0, \ t > 0.
\end{aligned}
$$

For $h_1, h_2 \in C([0, x_l], \mathbb{R}_+)$, we consider the following linear parabolic system

$$
\begin{aligned}
&\bar{I}_t = d_p \bar{I}_{xx} + \omega \bar{I}_x + b\beta e^{-(\omega/d_p)x} h_1 V - \delta \bar{I}, \ x \in (0, x_l), \ t > 0, \\
&V_t = d_v V_{xx} + q\delta e^{(\omega/d_p)x} \bar{I} - \mu_v V - \beta h_2 V, \ x \in (0, x_l), \ t > 0, \quad (3.20) \\
&\bar{I}_x(0, t) = \bar{I}_x(x_l, t) = V_x(0, t) = V_x(x_l, t) = 0, \ t > 0.
\end{aligned}
$$

Let $\Theta^{h_2}(t) : C([0, x_l], \mathbb{R}^2) \to C([0, x_l], \mathbb{R}^2)$ denote the solution semigroup generated by the following system

$$
\begin{aligned}
&\bar{I}_t = d_p \bar{I}_{xx} + \omega \bar{I}_x - \delta \bar{I}, \ x \in (0, x_l), \ t > 0, \\
&V_t = d_v V_{xx} + q\delta e^{(\omega/d_p)x} \bar{I} - (\mu_v + \beta h_2)V, \ x \in (0, x_l), \ t > 0, \\
&\bar{I}_x(0, t) = \bar{I}_x(x_l, t) = V_x(0, t) = V_x(x_l, t) = 0, \ t > 0.
\end{aligned}
$$

Define

$$
F^{h_1}(x) = \begin{pmatrix} 0 & b\beta e^{-(\omega/d_p)x} h_1 \\ 0 & 0 \end{pmatrix}.
$$

We assume that the distribution of initial infected phytoplankton and free lytic viruses is $\rho(x) = (\rho_1(x), \rho_2(x))$. As time evolves, the distribution at time t is $\Theta^{h_2}(t)\rho(x)$. Therefore, it can be deduced that the distribution of total new infected phytoplankton is

$$
K^{h_1, h_2}(\rho)(x) = \int_0^\infty F^{h_1}(x)\Theta^{h_2}(t)\rho(x)dt.
$$

Here K^{h_1,h_2} is called the next generation operator, and its spectral radius is $r(K^{h_1,h_2})$. It follows that the basic reproduction number associated with (h_1, h_2) is given as

$$R_0(h_1, h_2) := r(K^{h_1,h_2}). \tag{3.21}$$

Especially, if $h_1 = h_2 = S_2$, then the basic reproduction number associated with E_2 for virus transmission is denoted as

$$R_0 := R_0(S_2, S_2) = r(K^{S_2,S_2}). \tag{3.22}$$

Since the uniqueness of E_2 is not known, R_0 defined in (3.22) depends on E_2, and the definition given in (3.21) allows a more general basic reproduction number which will be used in the following.

Let $\bar{I} = e^{\lambda t}\varphi$ and $V = e^{\lambda t}\psi$. Then (λ, φ, ψ) satisfies an eigenvalue problem

$$\begin{aligned}
\lambda\varphi &= d_p\varphi_{xx} + \omega\varphi_x + b\beta e^{-(\omega/d_p)x}h_1\psi - \delta\varphi, \ x \in (0, x_l), \\
\lambda\psi &= d_v\psi_{xx} + q\delta e^{(\omega/d_p)x}\varphi - \mu_v\psi - \beta h_2\psi, \ x \in (0, x_l), \\
\varphi'(0) &= \varphi'(x_l) = \psi'(0) = \psi'(x_l) = 0.
\end{aligned} \tag{3.23}$$

Note that (3.23) is a cooperative system. By the Krein-Rutman theorem, (3.23) has a unique principal eigenvalue $\lambda_0(h_1, h_2)$ with a strongly positive eigenfunction $(\hat{\varphi}, \hat{\psi})$. Applying the similar arguments of Theorem 3.1 (i) in Wang and Zhao (2012), one can obtain the following conclusion.

Lemma 3.7 $\lambda_0(h_1, h_2)$ and $R_0(h_1, h_2) - 1$ have the same sign.

To apply the uniform persistence theory in Magal and Zhao (2005); Smith and Zhao (2001); Zhao (2017), we consider the susceptible phytoplankton-nutrient model (3.16) (the sub-system of (2.1)–(2.3) with $I = V = 0$).

Let

$$\begin{aligned}
\mathcal{U} &:= \{(S, N) \in C([0, x_l], \mathbb{R}^2) : S(x) \geq 0, \ N(x) \geq 0 \text{ on } [0, x_l]\}, \\
\mathcal{U}^* &:= \{(S, N) \in \mathcal{U} : S(\cdot) \not\equiv 0\}.
\end{aligned}$$

Denote the solution semiflow $\Sigma(t) : \mathcal{U} \to \mathcal{U}$ of (3.16) as

$$\Sigma(t)(u_0)(x) = (S(x, t, u_0), N(x, t, u_0)), \ x \in [0, x_l], \ t \geq 0,$$

where $(S(\cdot, t, u_0), N(\cdot, t, u_0))$ is the solution of (3.16) with the initial value $u_0 = (S_0, N_0) \in \mathcal{U}$. Following Lemmas 3.7 and 3.8 in Yan et al. (2022), one can obtain the following conclusion.

Lemma 3.8 If $R_p > 1$, then (3.16) has a global attractor Δ_0 in $\mathcal{U}^*$ satisfying $\Sigma(t)(\Delta_0) = \Delta_0$ and $(S_2, N_2) \in \Delta_0 \subset \text{Int}(C([0, x_l], \mathbb{R}_+^2)$.

From Theorem 3.3, we have $\lim_{t\to\infty}(S(\cdot,t),N(\cdot,t))=(0,N^0)$ when $R_p<1$. The numerical simulations in the next section suggest that the attractor Δ_0 when $R_p>1$ only contains the steady state (S_2,N_2).

Let

$$\mathcal{W}^* := \{(S,I,V,N)\in\mathcal{W}:S(\cdot)\not\equiv 0,\ I(\cdot)\not\equiv 0\ \text{and}\ V(\cdot)\not\equiv 0\}$$
$$\text{and } \partial\mathcal{W}^* := \mathcal{W}\setminus\mathcal{W}^*. \tag{3.24}$$

Here $\mathcal{W}$ is defined in (3.1). For any $(S,N)\in\mathcal{U}$, we introduce a projection $\mathcal{H}$ by $\mathcal{H}(S,N)=S$. Let

$$\Lambda_0=\mathcal{H}(\Delta_0),\ \ S_*(x)=\inf_{S\in\Lambda_0}S(x),\ \ S^*(x)=\sup_{S\in\Lambda_0}S(x)\ \text{for any}\ x\in[0,x_l].$$
$$\tag{3.25}$$

The uniform persistence shown in Lemma 3.8 implies that $0<S_*(x)\leq S^*(x)$ for $x\in[0,x_l]$ Substituting $h_1=S_*$, $h_2=S^*$ in (3.20) and (3.23) respectively, we can define the principal eigenvalue $\lambda_0(S_*,S^*)$ and the basic reproduction number $R_0(S_*,S^*)$ associated with (S_*,S^*). It follows from Lemma 3.7 that $\lambda_0(S_*,S^*)$ and $R_0(S_*,S^*)-1$ have the same sign.

Let $\Upsilon_0:=\{(S,0,0,N)\in\mathcal{W}:(S,N)\in\Delta_0\}$. It will prove that E_1 and Υ_0 are uniform weak repellers with respect to $\mathcal{W}^*$.

Lemma 3.9 *If $R_p>1$, then E_1 is a uniform weak repeller for (2.1)–(2.3) with respect to $\mathcal{W}^*$, that is, there is a $\upsilon_1>0$ satisfying $\limsup_{t\to\infty}\mathrm{dist}(\Theta(t)\sigma_0,E_1)\geq\upsilon_1$ for any $\sigma_0=(S_0,I_0,V_0,N_0)\in\mathcal{W}^*$.*

Proof If $R_p>1$, there is an $\epsilon>0$ satisfying $R_p^\epsilon=\mu_p^*/(\mu_p+\epsilon)>1$. Note that both f and g are continuous. Thus, for the above $\epsilon>0$, there is a $\upsilon_1>0$ such that

$$rg(N)f(L(x,S+\theta I))-\eta(S+\theta I)S-b\beta SV>rg(N^0)f(L(x,0))-\epsilon$$
$$\tag{3.26}$$

when $\|(S,I,V,N)-(0,0,0,N^0)\|<\upsilon_1$ on $[0,x_l]$. By (3.9), $\mu_p^*-\mu_p-\epsilon>0$ is the principal eigenvalue of

$$\lambda\xi=d_p\xi''-\omega\xi'+(rg(N^0)f(L(x,0))-\mu_p-\epsilon)\xi,\ x\in(0,x_l),$$
$$d_p\xi'(0)-\omega\xi(0)=d_p\xi'(x_l)-\omega\xi(x_l)=0$$

with the positive eigenvalue function $\xi^\epsilon(x)$.

Assume that the conclusion is not true. Then we can find a $\sigma_0\in\mathcal{W}^*$ satisfying

$$\limsup_{t\to\infty}\|\Theta(t)\sigma_0-(0,0,0,N^0)\|<\upsilon_1. \tag{3.27}$$

This suggests that

$$\|(S(\cdot, t, \sigma_0), I(\cdot, t, \sigma_0), V(\cdot, t, \sigma_0), N(\cdot, t, \sigma_0)) - (0, 0, 0, N^0)\| < \upsilon_1, \ t \geq T_1$$

for some sufficiently large T_1. It follows from the strong maximum principle and the Hopf boundary lemma that $S(\cdot, T_1, \sigma_0) > 0$ since $\sigma_0 \in \mathcal{W}^*$. Hence, there exists a $c_1 > 0$ such that $S(\cdot, T_1, \sigma_0) \geq c_1 \xi^\epsilon(\cdot)$. Let $\hat{S} = S e^{-(\omega/d_p)x}$ and $\hat{\xi}^\epsilon = \xi^\epsilon e^{-(\omega/d_p)x}$. From (3.26) and the S-equation in (2.1), we have

$$\hat{S}_t \geq d_p \hat{S}_{xx} + \omega \hat{S}_x + (rg(N^0)f(L(x, 0)) - \mu_p - \epsilon)\hat{S}, \ x \in (0, x_l), \ t > T_1,$$
$$\hat{S}_x(0, t) = \hat{S}_x(x_l, t) = 0, \ t \geq T_1,$$
$$\hat{S}(x, T_1, \sigma_0) \geq c_1 \hat{\xi}^\epsilon(x), \ x \in [0, x_l].$$

It is easy to see that $c_1 e^{(\mu_p^* - \mu_p - \epsilon)(t - T_1)} \hat{\xi}^\epsilon(x)$ is a solution of

$$\hat{S}_t = d_p \hat{S}_{xx} + \omega \hat{S}_x + (rg(N^0)f(L(x, 0)) - \mu_p - \epsilon)\hat{S}, \ x \in (0, x_l), \ t > T_1,$$
$$\hat{S}_x(0, t) = \hat{S}_x(x_l, t) = 0, \ t \geq T_1,$$
$$\hat{S}(x, T_1) = c_1 \hat{\xi}^\epsilon(x), \ x \in [0, x_l].$$

From the comparison theorem of parabolic system, we obtain

$$\hat{S}(\cdot, t, \sigma_0) \geq c_1 e^{(\mu_p^* - \mu_p - \epsilon)(t - T_1)} \hat{\xi}^\epsilon(\cdot)$$

for any $t \geq T_1$. Then $\lim_{t \to \infty} S(\cdot, t, \sigma_0) = \lim_{t \to \infty} \hat{S}(\cdot, t, \sigma_0)e^{(\omega/d_p)x} = \infty$ since $R_p^\epsilon > 1$. It contradicts (3.27). Therefore, E_1 is a uniform weak repeller with respect to $\mathcal{W}^*$. $\square$

Lemma 3.10 *Let S_* and S^* be defined as in (3.25). If $R_p > 1$ and $R_0(S_*, S^*) > 1$, then Υ_0 is a uniform weak repeller for (2.1)–(2.3) with respect to $\mathcal{W}^*$, that is, there is a $\upsilon_2 > 0$ satisfying $\limsup_{t \to \infty} \mathrm{dist}(\Theta(t)\sigma_0, \Upsilon_0) \geq \upsilon_2$ for any $\sigma_0 = (S_0, I_0, V_0, N_0) \in \mathcal{W}^*$.*

Proof If $R_0(S_*, S^*) > 1$, then $\lambda_0(S_*, S^*) > 0$. This indicates that there exists a $\upsilon_2 > 0$ such that $\lambda_0(S_* - \upsilon_2, S^* + \upsilon_2) > 0$ is the principal eigenvalue of

$$\lambda\varphi = d_p\varphi_{xx} + \omega\varphi_x + b\beta e^{-(\omega/d_p)x}(S_* - \upsilon_2)\psi - \delta\varphi, \ x \in (0, x_l), \ t > 0,$$
$$\lambda\psi = d_v\psi_{xx} + q\delta e^{(\omega/d_p)x}\varphi - \mu_v\psi - \beta(S^* + \upsilon_2)\psi, \ x \in (0, x_l), \ t > 0,$$
$$\varphi_x(0, t) = \varphi_x(x_l, t) = \psi_x(0, t) = \psi_x(x_l, t) = 0, \ t > 0$$

with the positive eigenvalue function $(\hat{\varphi}^{\upsilon_2}, \hat{\psi}^{\upsilon_2})$.

If the conclusion does not hold, then for the above υ_2, there exists a $\sigma_0 \in \mathcal{W}^*$ satisfying $\limsup_{t \to \infty} \mathrm{dist}(\Theta(t)\sigma_0, \Upsilon_0) < \upsilon_2$. This means that

$$\limsup_{t \to \infty} \mathrm{dist}(S(\cdot, t, \sigma_0), \Lambda_0) < \upsilon_2, \ \limsup_{t \to \infty} \|I(\cdot, t, \sigma_0)\| < \upsilon_2,$$
$$\limsup_{t \to \infty} \|V(\cdot, t, \sigma_0)\| < \upsilon_2 \tag{3.28}$$

and then there is a $T_2 > 0$ such that

$$\text{dist}(S(\cdot, t, \sigma_0), \Lambda_0) < \upsilon_2 \text{ for all } t \geq T_2.$$

Since Λ_0 is compact, we can find an $\bar{S}^t \in \Lambda_0$ satisfying

$$\|S(\cdot, t, \sigma_0) - \bar{S}^t(\cdot)\| < \upsilon_2 \text{ for all } t \geq T_2.$$

Hence,

$$S_*(\cdot) - \upsilon_2 \leq \bar{S}^t(\cdot) - \upsilon_2 < S(\cdot, t, \sigma_0) < \bar{S}^t(\cdot) + \upsilon_2 \leq S^*(\cdot) + \upsilon_2 \text{ for all } t \geq T_2.$$

From the I- and V-equations in (2.1), we let $\bar{I} = I e^{-(\omega/d_p)x}$ and have

$$\bar{I}_t \geq d_p \bar{I}_{xx} + \omega \bar{I}_x + b\beta e^{-(\omega/d_p)x}(S_* - \upsilon_2)V - \delta \bar{I}, \ x \in (0, x_l), \ t > T_2,$$
$$V_t \geq d_v V_{xx} + q\delta e^{(\omega/d_p)x}\bar{I} - \mu_v V - \beta(S^* + \upsilon_2)V, \ x \in (0, x_l), \ t > T_2,$$
$$\bar{I}_x(0, t) = \bar{I}_x(x_l, t) = V_x(0, t) = V_x(x_l, t) = 0, \ t > T_2.$$

By the strong maximum principle and the Hopf boundary lemma, $\bar{I}(x, T_2, \sigma_0) > 0$ and $V(x, T_2, \sigma_0) > 0$ for $\sigma_0 \in \mathcal{W}^*$. There is a $c_2 > 0$ satisfying $(\bar{I}(x, T_2, \sigma_0), V(x, T_2, \sigma_0)) \geq c_2(\hat{\varphi}^{\upsilon_2}, \hat{\psi}^{\upsilon_2})$ on $x \in [0, x_l]$. It can be seen that $c_2 e^{\lambda_0(S_* - \upsilon_2, S^* + \upsilon_2)(t - T_2)}(\hat{\varphi}^{\upsilon_2}, \hat{\psi}^{\upsilon_2})$ is a solution of

$$\bar{I}_t = d_p \bar{I}_{xx} + \omega \bar{I}_x + b\beta e^{-(\omega/d_p)x}(S_* - \upsilon_2)V - \delta \bar{I}, \ x \in (0, x_l), \ t > T_2,$$
$$V_t = d_v V_{xx} + q\delta e^{(\omega/d_p)x}\bar{I} - \mu_v V - \beta(S^* + \upsilon_2)V, \ x \in (0, x_l), \ t > T_2,$$
$$\bar{I}_x(0, t) = \bar{I}_x(x_l, t) = V_x(0, t) = V_x(x_l, t) = 0, \ t > T_2.$$

Applying the comparison theorem of parabolic system again, we have

$$(\bar{I}(x, t, \sigma_0), V(x, t, \sigma_0)) \geq c_2 e^{\lambda_0(S_* - \upsilon_2, S^* + \upsilon_2)(t - T_2)}(\hat{\varphi}^{\upsilon_2},$$
$$\hat{\psi}^{\upsilon_2}) \text{ for all } x \in [0, x_l], \ t \geq T_2.$$

This implies that $\bar{I}(x, t, \sigma_0), V(x, t, \sigma_0)$ are unbounded since $\lambda_0(S_* - \upsilon_2, S^* + \upsilon_2) > 0$. This contradicts with (3.28). The proof is completed. □

Now we are ready to prove the existence of E_3 and uniform persistence of model (2.1)–(2.3) when $R_p > 1$ and $R_0(S_*, S^*) > 1$.

Theorem 3.11 *Let S_* and S^* be defined as in (3.25). If $R_p > 1$ and $R_0(S_*, S^*) > 1$, then model (2.1)–(2.3) is uniformly persistent for $(\mathcal{W}^*, \partial\mathcal{W}^*)$, that is, there exists a $\upsilon > 0$ satisfying*

$$\liminf_{t \to \infty} S(\cdot, t, \sigma_0) > \upsilon, \ \liminf_{t \to \infty} I(\cdot, t, \sigma_0) > \upsilon, \ \liminf_{t \to \infty} V(\cdot, t, \sigma_0) > \upsilon \quad (3.29)$$

for any $\sigma_0 = (S_0, I_0, V_0, N_0) \in \mathcal{W}^*$. Moreover, model (2.1)–(2.3) possesses at least one endemic steady state E_3.

Proof Applying the Hopf boundary lemma and strong maximum principle again, one can obtain

$$S(\cdot, t, \sigma_0) > 0, \ I(\cdot, t, \sigma_0) > 0, \ V(\cdot, t, \sigma_0) > 0, \ N(\cdot, t, \sigma_0) > 0 \qquad (3.30)$$

for any $t > 0$ and $\sigma_0 \in \mathcal{W}^*$, where $\mathcal{W}^*$ is defined in (3.24). Thus, $\mathcal{W}^*$ is positively invariant under $\Theta(t)$. Set $M_\partial := \{\sigma_0 \in \partial\mathcal{W}^* : \Theta(t)\sigma_0 \in \partial\mathcal{W}^* \text{ for any } t \geq 0\}$ and let $\omega(\sigma_0)$ be the omega limit set of the forward orbit $O^+(\sigma_0) := \{\Theta(t)\sigma_0 : t \geq 0\}$.

We claim that $\omega(\sigma_0) \subset E_1 \cup \Upsilon_0$ for any $\sigma_0 \in M_\partial$. Note that $\Theta(t)\sigma_0 \in M_\partial$ for any fixed $\sigma_0 \in M_\partial$. This implies that $S(\cdot, t, \sigma_0) \equiv 0$ or $I(\cdot, t, \sigma_0) \equiv 0$ or $V(\cdot, t, \sigma_0) \equiv 0$ for $\sigma_0 \in M_\partial$. The I and V equations in (2.1) are a cooperative system. Hence, $I(\cdot, t, \sigma_0) \equiv 0$ if and only if $V(\cdot, t, \sigma_0) \equiv 0$. This means that we only need to investigate the following three cases:
(i) if $S_0 \equiv 0, V_0 \equiv 0$, then $S(\cdot, t, \sigma_0) \equiv 0$ for any $t \geq 0$ from the uniqueness of solutions. The I-equation in model (2.1) reduces to

$$I_t = d_p I_{xx} - \omega I_x - \delta I, \ x \in (0, x_l), \ t > 0,$$
$$d_p I_x(0, t) - \omega I(0, t) = d_p I_x(x_l, t) - \omega I(x_l, t) = 0, \ t > 0.$$

Similar to the derivation process in (3.13)–(3.15), we have

$$\limsup_{t \to \infty} I(\cdot, t, \sigma_0) = 0, \ \limsup_{t \to \infty} V(\cdot, t, \sigma_0) = 0 \text{ and } \limsup_{t \to \infty} N(\cdot, t, \sigma_0) = N_0.$$

Thus, $\omega(\sigma_0) = E_1$.
(ii) if $S_0 \equiv 0, V_0 \neq 0$, then $S(\cdot, t, \sigma_0) \equiv 0$. Similar to case (i), we have $\omega(\sigma_0) = E_1$.
(iii) if $S_0 \neq 0, V_0 \equiv 0$, then $\limsup_{t \to \infty} I(\cdot, t, \sigma_0) = 0$ and $\limsup_{t \to \infty} V(\cdot, t, \sigma_0) = 0$ from (3.13) and (3.14). By the theory of asymptotic autonomous systems (see Theorem 1.8 in Mischaikow et al. 1995 or Theorem 4.1 in Thieme 1992), (2.1) reduces to (3.16). From Lemma 3.8, $(S(\cdot, t, u_0), N(\cdot, t, u_0))$ will eventually enter Δ_0. Hence $\omega(\sigma_0) \subset \Upsilon_0$.

By Lemmas 3.9 and 3.10, E_1 and Υ_0 are uniform weak repellers for $\mathcal{W}^*$. To obtain our conclusion, we let $\varpi : \mathcal{W} \to [0, \infty)$ satisfying

$$\varpi(\sigma_0) := \min\left\{\min_{x \in [0, x_l]} S_0(x), \ \min_{x \in [0, x_l]} I_0(x), \ \min_{x \in [0, x_l]} V_0(x)\right\}$$
$$\text{for any } \sigma_0 = (S_0, I_0, V_0, N_0) \in \mathcal{W}.$$

By (3.30), we get $\varpi^{-1}(0, \infty) \subseteq \mathcal{W}^*$ and $\varpi(\Theta(t)\sigma_0) > 0$ for any $t > 0$ if $\varpi(\sigma_0) > 0$ or $\sigma_0 \in \mathcal{W}^*$ with $\varpi(\sigma_0) = 0$. For the semiflow $\Theta(t) : \mathcal{W} \to \mathcal{W}$, ϖ is a generalized distance function. In view of the above analysis, we conclude that $\omega(\sigma_0) \subset E_1 \cup \Upsilon_0$ for any $\sigma_0 \in M_\partial$, and there is no cycle in M_∂ from $E_1 \cup \Upsilon_0$ to $E_1 \cup \Upsilon_0$. Furthermore, E_1 and Υ_0 are isolated in $\mathcal{W}$. Let $W^s(E_1)$ and $W^s(\Upsilon_0)$ denote the stable sets of E_1 and Υ_0 respectively. It is easy to see that $W^s(E_1) \cap \mathcal{W}^* = \emptyset$ and $W^s(\Upsilon_0) \cap \mathcal{W}^* = \emptyset$. From Remark 3.2, $\Theta(t)$ has a global attractor in $\mathcal{W}$. By Theorem 3 in Smith and
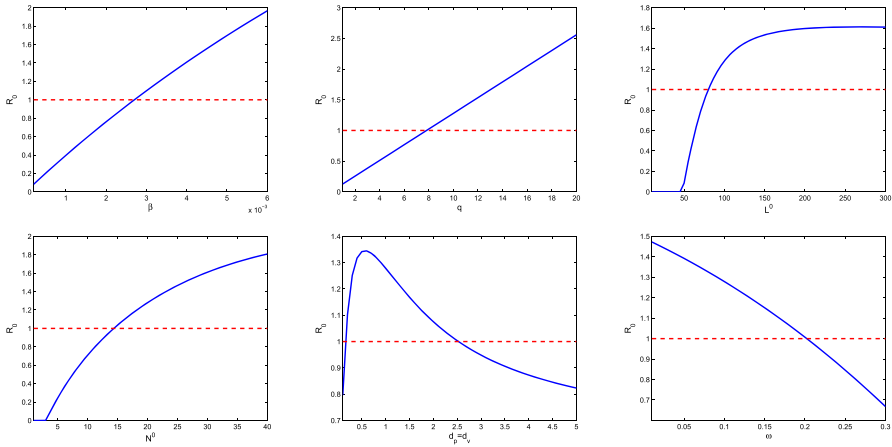
Fig. 2 Dependence of R_0 on some model parameters. Here $L^0 = 100$, $N^0 = 20$ and the remaining parameter values are derived from Table 1

Zhao (2001), there exists a $\upsilon > 0$ such that $\min\limits_{\phi \in \omega(\sigma_0)} \varpi(\phi) > \upsilon$ for any $\sigma_0 \in \mathcal{W}^*$. It follows that (3.29) holds and the uniform persistence is valid. Applying Theorem 3.7 and Remark 3.10 in Magal and Zhao (2005), $\Theta(t) : \mathcal{W}^* \to \mathcal{W}^*$ admits a global attractor. By Theorem 4.7 in Magal and Zhao (2005), model (2.1)–(2.3) has at least one endemic steady state $E_3 \in \mathcal{W}^*$. Similar to the proof in Lemma 3.5, we have $S_3(x) > 0$, $N_3(x) > 0$ on $[0, x_l]$. Let $\bar{I}_3 = I_3 e^{-(\omega/d_p)x}$. From the second and third equalities in (3.7), we obtain

$$-d_p \bar{I}_3'' - \omega \bar{I}_3' + \delta \bar{I}_3 = b\beta S_3 V_3 e^{-(\omega/d_p)x} \geq 0, \ x \in (0, x_l), \ \bar{I}_3(0) = \bar{I}_3(x_l) = 0$$

and

$$-d_v V_3''(x) + (\mu_v + \beta S_3)V_3 = q\delta I_3 \geq 0, \ x \in (0, x_l), \ V_3'(0) = V_3'(x_l) = 0.$$

Thus, $I_3(x) > 0$ and $V_3(x) > 0$ on $[0, x_l]$ following the strong maximum principle. The proof is complete. □

From numerical simulations, we speculate that the global attractor $\Delta_0 = \{(S_2, N_2)\}$ in Lemma 3.8 and the basic reproduction number $R_0(S_*, S^*) = R_0(S_2, S_2) = R_0$ can be uniquely determined. Theorem 3.11 shows that lytic viruses will be transmitted in the phytoplankton population if $R_p > 1$ and $R_0 > 1$. Hence $R_0 = 1$ is a threshold for lytic viruses from persistence to extinction. Figure 2 reveals the evolution of R_0 with respect to model parameters. From numerical simulations in Sect. 3.3, the detailed lytic virus transmission is more complicated. The endemic state may be a positive steady state E_3, or a positive spatially inhomogeneous periodic solution.
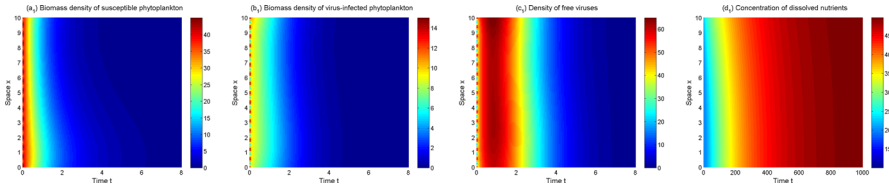
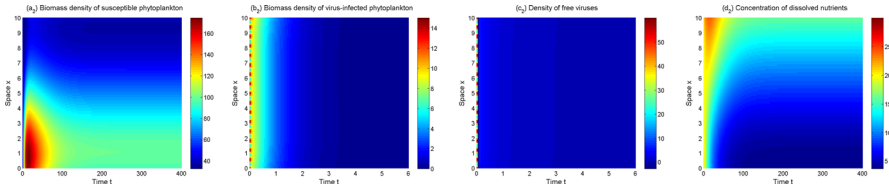**Fig. 3** The solutions of model (2.1)–(2.3) converge to E_1 for $\mu_p = 1, \mu_v = 1.2$

Fig. 4 The solutions of model (2.1)–(2.3) converge to E_2 for $\mu_p = 0.1, \mu_v = 24$
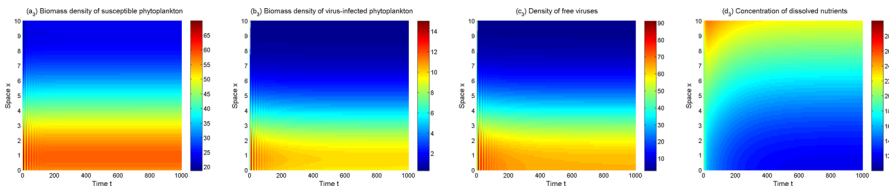

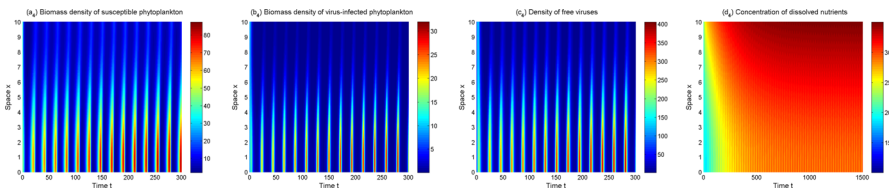**Fig. 5** The solutions of model (2.1)–(2.3) converge to E_3 for $\mu_p = 0.1, \mu_v = 1.6$

Fig. 6 The solutions of model (2.1)–(2.3) converge to a positive spatially inhomogeneous periodic solution for $\mu_p = 0.1, \mu_v = 0.6$

3.3 Simulations

In view of the above model analysis, we do some numerical simulations to further describe dynamics of the model (2.1)–(2.3). From Figs. 3, 4, 5 and 6, one can observe that the solutions of model (2.1)–(2.3) converge to different asymptotic states for different μ_p, μ_v. Here ecologically reasonable parameter values are from Table 1 and the initial conditions are $S_0(x) = 40 + 5\sin x, I_0(x) = 10 + 5\cos x, V_0(x) = 40 + 20\cos x, N_0(x) = 20 + 10\sin x$ on [0, 10].

In Fig. 3, the extinct steady state E_1 is the attractor with $R_p = 0.49$. Phytoplankton are extinct and thus the lytic virus does not spread in the water column. Nutrients tend to the input concentration N^0 and are spatially uniformly distributed. Figure 4 shows that the (possibly unique) disease-free steady state E_2 is the attractor when $R_p =$

4.91 and $R_0 = 0.13$. Phytoplankton invade aquatic ecosystems and exhibit vertical aggregation. Lytic virus still cannot be transmitted among phytoplankton because lytic virus mortality is high.

The model (2.1)–(2.3) is uniformly persistent and an endemic steady state E_3 appears to be the asymptotic state when $R_p = 4.91$ and $R_0 = 1.59$ (see Fig. 5). As μ_v decreases further ($R_p = 4.91$, $R_0 = 3.24$), a positive spatially inhomogeneous periodic solution becomes the asymptotic state, which arises from bifurcate from E_3 via a Hopf bifurcation (see Fig. 6). Both Figs. 5 and 6 show the lytic virus is prevalent in the phytoplankton, either in a form of spatially heterogenous steady state (Fig. 5) or a spatially heterogenous temporal-oscillatory fashion (Fig. 6). It is noticeable that susceptible phytoplankton, virus-infected phytoplankton and lytic viruses aggregate near the water surface (for only short time in the oscillatory case). Comparing Fig. 4 (a_2)–(b_2) and Fig. 5 (a_3)–(b_3), one can also observe that lytic viruses reduce phytoplankton biomass.

4 Phytoplankton blooms and lytic virus transmission

Phytoplankton blooms are an important manifestation of the pollution of the aquatic environments, and even lead to the collapse of entire aquatic ecosystems. It has been shown that the wide spreading of lytic viruses transmission among phytoplankton can control phytoplankton blooms from observations and experiments (Fuhrman 1999; Kuhlisch et al. 2021). In the following discussion, we will verify these observations and experimental results with the proposed model (2.1)–(2.3). It is noted that the role of ecological factors in the interaction of phytoplankton blooms and lytic virus transmission is not very clear. It is also necessary and significant to explore the effects of ecological factors in this process.

We focus on the environmental parameters related to viral transmission and ecological factors in model (2.1)–(2.3). Those parameters include viral infection-related rates β, q, spatial ecological factors d_p, d_v, d_n, ω, and resource-related ecological factors L^0 and N^0. In the figures below, we show the evolution of asymptotic states (steady state solutions E_1, E_2, E_3 and the spatially inhomogeneous periodic solution) for different parameter values. When the solutions of (2.1)–(2.3) converge to one of E_1, E_2, E_3 or the spatially inhomogeneous periodic solution, numerical bifurcation diagrams show the evolution trend of densities of susceptible phytoplankton $((1/x_l) \int_0^{x_l} S(x)dx)$, virus-infected phytoplankton $((1/x_l) \int_0^{x_l} I(x)dx)$, and free lytic viruses $((1/x_l) \int_0^{x_l} V(x)dx)$. For the time-periodic solutions, the minimum and maximum values are shown. Time series diagrams reveal the evolution of densities of susceptible phytoplankton $(((1/x_l) \int_0^{x_l} S(x, t)dx)$, infected phytoplankton $((1/x_l) \int_0^{x_l} I(x, t)dx)$ and lytic viruses $((1/x_l) \int_0^{x_l} V(x, t)dx)$ over time. The parameter values of the numerical analysis used here are derived from Table 1. The simulations are implemented in MATLAB via the finite difference method.

We first examine the effect of lytic virus transmission parameters β, q. Changes in these parameters are closely related to ecological factors such as temperature, salinity (Demory et al. 2021). The transmission coefficient β is an important indicator for
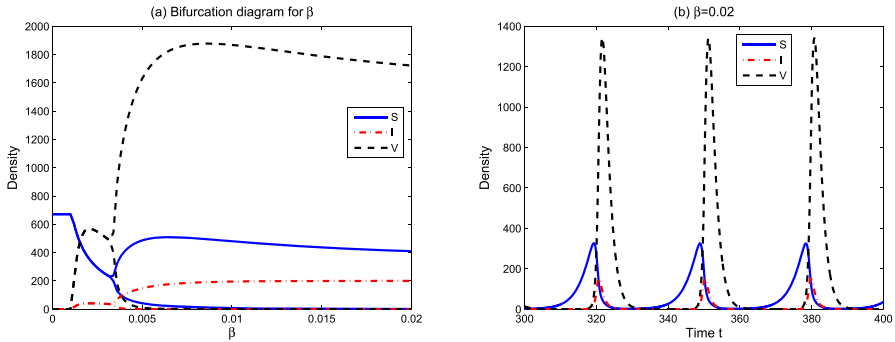
Fig. 7 **a** Effect of the transmission coefficient β on the density of susceptible phytoplankton, virus-infected phytoplankton and lytic viruses. **b** Time series of density of phytoplankton and viruses

assessing host resistance to infection. Figure 7 displays the variation of phytoplankton and lytic virus densities in model (2.1)–(2.3) with the transmission coefficient β. For $\beta = 0$, one can observe that lytic viruses do not spread among phytoplankton and that susceptible phytoplankton biomass is at a high level. When β increases, susceptible phytoplankton biomass gradually declines, while lytic virus loads ascend sharply and a significant proportion of phytoplankton are infected by viruses. In Fig. 7a, b, spatially inhomogeneous periodic solutions bifurcate from positive steady states through a Hopf bifurcation at $\beta = 0.0032$. This shows that increasing the transmission coefficient will lead to persistent phytoplankton blooms, but a large transmission coefficient will cause a large amplitude pulse bloom which occurs periodically about every thirty days. In the latter case, an increase of susceptible phytoplankton precedes the peak of virus transmission, then the phytoplankton population is at a low level for a long time until the next wave.

The lytic virus burst size varies with host genotype or environmental conditions. It is an important factor for describing the transmission of lytic viruses among phytoplankton (Edwards and Steward 2018). Figure 8 shows an evolution of asymptotic states in model (2.1)–(2.3) for varying burst size q similar to the one for transmission coefficient. The dynamics of the model progress from a disease-free steady state, to an endemic steady state, and then to a spatially inhomogeneous periodic solution. This indicates that the small burst size does not cause phytoplankton infection and that only a certain degree of burst size can lead to the spread of lytic viruses among phytoplankton and a decrease in total phytoplankton biomass.

Emiliana huxleyi are eukaryotic microscopic phytoplankton that are widely distributed in oceans or brackish waters. They are one of the important producers in marine ecosystems, especially playing an important role in the carbon cycle of oceans. E*miliana huxleyi* have frequent, large-scale blooms each year. It is known that *Emiliana huxleyi* can be massively infected by a lytic virus with a large double-stranded DNA structure. The lytic virus is called *Emiliana huxleyi* virus and causes massive mortality of *Emiliana huxleyi*. In Fuhrman (1999); Kuhlisch et al. (2021), the authors stated that *Emiliana huxleyi* blooms are often terminated by *Emiliana huxleyi* virus from experiments and observations.
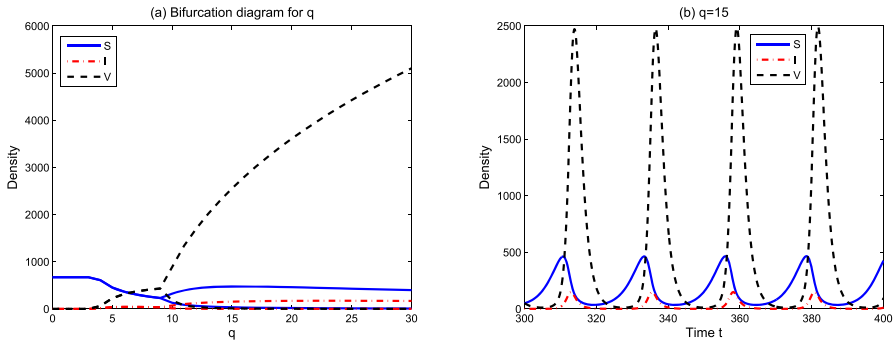
Fig. 8 **a** Effect of the burst size q on the density of susceptible phytoplankton, virus-infected phytoplankton and lytic viruses. **b** Time series of density of phytoplankton and viruses
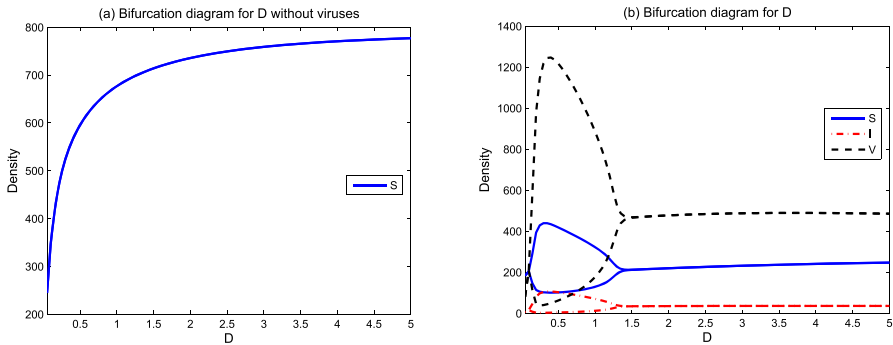

Fig. 9 Effect of the vertical turbulent diffusivity $D = d_p = d_v = d_n$ on the density of susceptible phytoplankton, virus-infected phytoplankton and lytic viruses

The periodic pattern shown in Fig. 7b is consistent with the observations and experimental results of *Emiliana huxleyi*-lytic virus interactions in Fuhrman (1999); Kuhlisch et al. (2021). At the beginning of a bloom cycle, both phytoplankton and lytic virus densities are at a very low value. After that, the susceptible phytoplankton biomass rises rapidly and reaches a maximum, while the virus density remains almost constant. Phytoplankton blooms occur at this time. As the time progresses further, there is a sudden and dramatic increase in lytic virus density. This indicates a large-scale spread of lytic viruses among phytoplankton. During this process, the total phytoplankton biomass declines sharply. When the virus reaches its maximum, phytoplankton biomass tends to almost zero, thus the bloom ends. In the last stage of this bloom cycle, the viral density decreases, and is again at a low value together with phytoplankton. Figure 8b also exhibits a similar periodic bloom cycle pattern. The above findings effectively validate the large-scale transmission of lytic viruses to terminate phytoplankton blooms.

The evolution of phytoplankton and lytic virus densities with different spatial ecological factors (turbulent diffusivity and directional movement velocity) can be seen in Figs. 9 and 10. Phytoplankton, viruses, and nutrients all move randomly in the water column with turbulence, so it is assumed that they have the same diffusion coefficient $D = d_p = d_v = d_n$. If there are no viruses in the aquatic environment, the phytoplank-
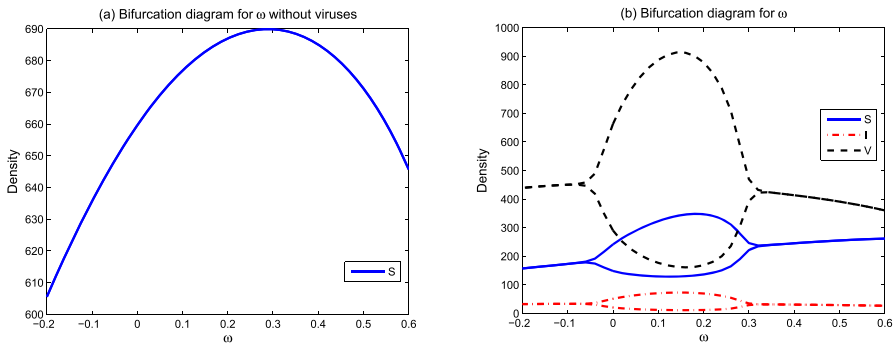
Fig. 10 Effect of the sinking or buoyant velocity ω on the density of susceptible phytoplankton, virus-infected phytoplankton and lytic viruses
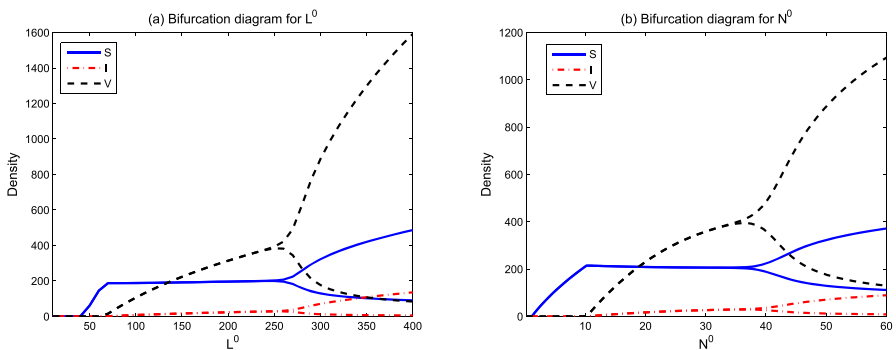

Fig. 11 Effects of the water surface light intensity L^0 and sediment input nutrient concentration N^0 on the density of susceptible phytoplankton, virus-infected phytoplankton and lytic viruses

ton biomass rises rapidly and reaches a high value with increasing turbulence intensity. It is because adequate nutrient transport in the water column facilitates better phytoplankton growth (see Fig. 9a). When the lytic virus spreads among phytoplankton, the biomass of phytoplankton, including susceptible and infected phytoplankton, remains almost unchanged for $D \in (0.02, 5)$ except the periodic oscillatory patterns occurring for the intermediate diffusion rate (see Fig. 9b). In this process, there are two stability switches from steady states to periodic oscillations, and then back to steady states. This illustrates that the presence of lytic viruses not only leads to complex dynamics, but also effectively reduces the phytoplankton biomass. Comparing Fig. 10a, b, similar conclusions are obtained for the directional movement velocity ω. This once again confirms that lytic virus transmission can effectively control phytoplankton blooms.

Light and nutrients are two important ecological factors, and their abundance directly affects the invasion of phytoplankton and the spread of lytic viruses. We choose the water surface light intensity L^0 and sediment nutrient input concentration N^0 as typical resource-related ecological factors to explore the survival and extinction of phytoplankton and lytic viruses. Figure 11 shows that low L^0 or N^0 causes phytoplankton extinction since light and nutrients are two essential resources for phy-
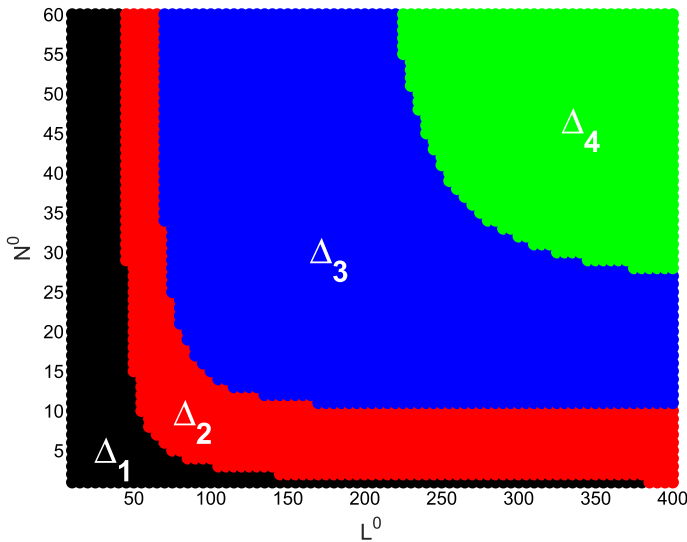
Fig. 12 Parameter regions of L^0 versus N^0 for the survival and extinction of phytoplankton and lytic viruses. Phytoplankton are extinct in Δ_1 ($R_p < 1$), phytoplankton survive while lytic viruses become extinct in Δ_2 ($R_p > 1$, $R_0 < 1$), lytic viruses spread among phytoplankton in a steady state form in Δ_3 ($R_p > 1$, $R_0 > 1$) or as a spatially inhomogeneous periodic solution form in Δ_4 ($R_p > 1$, $R_0 > 1$)

toplankton growth. With the gradual increase of L^0 or N^0, phytoplankton first invade aquatic ecosystems, after which lytic viruses begin to spread among phytoplankton. When L^0 or N^0 is at a high value, the system undergoes a Hopf bifurcation and exhibits periodic oscillations. This is a classical paradox of enrichment.

The combined effects of L^0 and N^0 are presented in Fig. 12. Using the basic ecological reproductive index R_p and basic reproduction number R_0 to distinguish dynamic behavior, we take L^0 and N^0 as the coordinate parameters to divide the first quadrant of the $L^0 - N^0$ plane into four regions Δ_i for $i = 1, 2, 3, 4$. Phytoplankton go extinct in Δ_1 ($R_p < 1$); Phytoplankton successfully invade aquatic habitats, while lytic viruses cannot survive in Δ_2 ($R_p > 1$ and $R_0 < 1$). If $R_p > 1$ and $R_0 > 1$, lytic viruses spread among phytoplankton as a steady state form in Δ_3 or as a spatially inhomogeneous periodic solution form in Δ_4. These findings suggest that it is very difficult for lytic viruses to spread in a low-light or oligotrophic aquatic ecosystem.

5 Conclusion and discussion

Viruses are pervasive components of aquatic ecosystems, and have important influences on aquatic biodiversity and biogeochemical cycles (Suttle 2005; Suttle et al. 1990). As one of the common viruses, lytic viruses use phytoplankton cells as their primary hosts and are ubiquitous in aquatic ecosystems (Demory et al. 2021; Edwards and Steward 2018; Fuhrman et al. 2011; Kuhlisch et al. 2021). They replicate and reproduce inside phytoplankton cells, and eventually release virions by lysing the

cells. The spread of lytic viruses causes a dramatic decrease in phytoplankton biomass and even terminates phytoplankton blooms. Few mathematical models have been formulated to explore the interactions between phytoplankton and lytic viruses and to expound the mechanisms of lytic virus transmission.

The dynamic model (2.1)–(2.3) is proposed to describe the spread of lytic virus among phytoplankton in a water column. Compared with the existing models in Béchette et al. (2013); Beretta and Kuang (1998); Demory et al. (2021); Edwards and Steward (2018); Fuhrman et al. (2011), there are two novel points in model (2.1)–(2.3). One is to consider a poorly mixed aquatic environment and take account of random movements of phytoplankton and viruses. The other is to add phytoplankton sinking movement and include light as a factor contributing to the growth of phytoplankton. Our results show that these newly added factors have a significant effect on the dynamics of phytoplankton growth and the spread of lytic viruses.

Two quantitative ecological indices: the basic ecological reproductive index R_p for phytoplankton invasion and the basic reproduction number R_0 for virus transmission, are rigorously derived from the model. According to Theorems 3.3, 3.6, 3.11 and corresponding remarks, phytoplankton go extinct if $R_p < 1$, phytoplankton successfully invade and lytic viruses are extinct if $R_p > 1$ and $R_0 < 1$, lytic viruses spread among phytoplankton as a steady state form or a spatially inhomogeneous periodic solution form if $R_p > 1$ and $R_0 > 1$. By using theoretical and numerical analysis of the model (2.1)–(2.3), we consider the interaction between phytoplankton blooms and lytic virus transmission and the role of ecological factors. From the numerical bifurcation diagrams (Figs. 7, 8, 9, 10, 11), one can observe that the spread of lytic viruses controls phytoplankton biomass. Time series diagrams (Figs. 7, 8b) reveal large-scale outbreaks of lytic virus infection effectively terminate phytoplankton blooms. The findings validate the observations and experimental results of *Emiliana huxleyi*-lytic virus interactions in Fuhrman (1999); Kuhlisch et al. (2021). The studies also indicate that it is very difficult for lytic viruses to spread in a low-light or oligotrophic aquatic environment (see Figs. 11, 12).

In this paper, we attempt to model the spread of lytic virus among phytoplankton, and the mechanism of lytic virus transmission and its relationship with phytoplankton blooms are explored. There are still many mathematical and biological problems worthy of further study. Mathematically, more dynamic properties of model (2.1)–(2.3) need to be rigorously investigated. For example, the uniqueness and stability of disease-free steady state E_2 and endemic steady state E_3, and the existence of spatially inhomogeneous periodic solutions. Biologically, the phytoplankton intracellular nutrient-to-carbon ratio in model (2.1)–(2.3) is assumed to be constant, but in reality, it is significantly variable (Loladze et al. 2000; Wang et al. 2007). It is desirable to include this factor in phytoplankton-virus interactions. Bacteria are a very important aquatic microorganism. They decompose organic carbon produced by phytoplankton and are infected by aquatic viruses (Fuhrman 1999; Suttle 2005; Wang et al. 2007; Yan et al. 2022). It is very natural to add bacteria into the model (2.1)–(2.3) and further explore the carbon cycle in aquatic ecosystems. In addition, the effects of zooplankton, fish (Chen et al. 2017) and toxins (Shan and Huang 2019; Nie et al. 2017) could also be considered.

Data availibility The datasets generated during and/or analyzed during the current study are available from the corresponding author on reasonable request.

Declarations

Conflict of interest The authors declare they have no conflict of interest.

References

Béchette A, Stojsavljevic T, Tessmer M, Berges JA, Pinter GA, Young EB (2013) Mathematical modeling of bacteria-virus interactions in Lake Michigan incorporating phosphorus content. J Great Lakes Res 39(4):646–654

Beretta E, Kuang Y (1998) Modeling and analysis of a marine bacteriophage infection. Math Biosci 149(1):57–76

Chen M, Fan M, Kuang Y (2017) Global dynamics in a stoichiometric food chain model with two limiting nutrients. Math Biosci 289:9–19

Chen M, Fan M, Liu R, Wang XY, Yuan X, Zhu HP (2015) The dynamics of temperature and light on the growth of phytoplankton. J Theor Biol 385:8–19

Crandall MG, Rabinowitz PH (1971) Bifurcation from simple eigenvalues. J Funct Anal 8(2):321–340

Crandall MG, Rabinowitz PH (1973) Bifurcation, perturbation of simple eigenvalues and linearized stability. Arch Rational Mech Anal 52(2):161–180

Davies CM, Wang H (2021) Incorporating carbon dioxide into a stoichiometric producer-grazer model. J Math Biol 83(5):1–48

Demory D, Weitz JS, Baudoux AC, Touzeau S, Simon N, Rabouille S, Sciandra A, Bernard O (2021) A thermal trade-off between viral production and degradation drives virus-phytoplankton population dynamics. Ecol Lett 24(6):1133–1144

Edwards KF, Steward GF (2018) Host traits drive viral life histories across phytoplankton viruses. Am Nat 191(5):566–581

Fuhrman JA (1999) Marine viruses and their biogeochemical and ecological effects. Nature 399(6736):541–548

Fuhrman KM, Pinter GA, Berges JA (2011) Dynamics of a virus-host model with an intrinsic quota. Math Comput Model 53(5–6):716–730

Gourley SA, Kuang Y (2004) A delay reaction–diffusion model of the spread of bacteriophage infection. SIAM J Appl Math 65(2):550–566

Grover JP (2017) Sink or swim? Vertical movement and nutrient storage in phytoplankton. J Theor Biol 432:38–48

Hale JK (1988) Asymptotic behavior of dissipative systems, vol 25. Mathematical Surveys and Monographs. American Mathematical Society, Providence, RI

Ho JC, Michalak AM, Pahlevan N (2019) Widespread global increase in intense lake phytoplankton blooms since the 1980s. Nature 574(7780):667–670

Hsu SB, Lam KY, Wang FB (2017) Single species growth consuming inorganic carbon with internal storage in a poorly mixed habitat. J Math Biol 75(6):1775–1825

Hsu SB, Lou Y (2010) Single phytoplankton species growth with light and advection in a water column. SIAM J Appl Math 70(8):2942–2974

Huisman J, Arrayás M, Ebert U, Sommeijer B (2002) How do sinking phytoplankton species manage to persist? Am Nat 159(3):245–254

Huisman J, Pham Thi NN, Karl DM, Sommeijer B (2006) Reduced mixing generates oscillations and chaos in the oceanic deep chlorophyll maximum. Nature 439(7074):322–325

Jäger CG, Diehl S (2014) Resource competition across habitat boundaries: asymmetric interactions between benthic and pelagic producers. Ecol Monogr 84(2):287–302

Jäger CG, Diehl S, Emans M (2010) Physical determinants of phytoplankton production, algal stoichiometry, and vertical nutrient fluxes. Am Nat 175(4):91–104

Klausmeier CA, Litchman E (2001) Algal games: the vertical distribution of phytoplankton in poorly mixed water columns. Limnol Oceanogr 46(8):1998–2007

Kuhlisch C, Schleyer G, Shahaf N, Vincent F, Schatz D, Vardi A (2021) Viral infection of algal blooms leaves a unique metabolic footprint on the dissolved organic matter in the ocean. Sci Adv 7(25):eabf4680

Loladze I, Kuang Y, Elser JJ (2000) Stoichiometry in producer-grazer systems: linking energy flow with element cycling. Bull Math Biol 62(6):1137–1162

Magal P, Zhao XQ (2005) Global attractors and steady states for uniformly persistent dynamical systems. SIAM J Math Anal 37(1):251–275

Martin RH, Smith HL (1990) Abstract functional-differential equations and reaction–diffusion systems. Trans Am Math Soc 321(1):1–44

Mischaikow K, Smith H, Thieme HR (1995) Asymptotically autonomous semiflows: chain recurrence and Lyapunov functions. Trans Am Math Soc 347(5):1669–1685

Nie H, Hsu SB, Grover JP (2016) Algal competition in a water column with excessive dioxide in the atmosphere. J Math Biol 72(7):1845–1892

Nie H, Hsu SB, Wu JH (2017) A competition model with dynamically allocated toxin production in the unstirred chemostat. Commun Pure Appl Anal 16(4):1373–1404

Pang DF, Nie H, Wu JH (2019) Single phytoplankton species growth with light and crowding effect in a water column. Discrete Cont Dyn Syst 39(1):41–74

Ryabov AB, Rudolf L, Blasius B (2010) Vertical distribution and composition of phytoplankton under the influence of an upper mixed layer. J Theor Biol 263(1):120–133

Shan CH, Huang QH (2019) Direct and indirect effects of toxins on competition dynamics of species in an aquatic environment. J Math Biol 78(3):739–766

Shi JP, Wang XF (2009) On global bifurcation for quasilinear elliptic systems on bounded domains. J Differ Equ. 246(7):2788–2812

Smith HL, Thieme HR (2012) Persistence of bacteria and phages in a chemostat. J Math Biol 64(6):951–979

Smith HL, Zhao XQ (2001) Robust persistence for semidynamical systems. Nonlinear Anal TMA 47(9):6169–6179

Suttle CA (2005) Viruses in the sea. Nature 437(7057):356–361

Suttle CA, Chan AM, Cottrell MT (1990) Infection of phytoplankton by viruses and reduction of primary productivity. Nature 347(6292):467–469

Thieme HR (1992) Convergence results and a poincaré-bendixson trichotomy for asymptotically autonomous differential equations. J Math Biol 30(7):755–763

Vasconcelos FR, Diehl S, Rodríguez P, Hedström P, Karlsson J, Byström P (2016) Asymmetrical competition between aquatic primary producers in a warmer and browner world. Ecology 97(10):2580–2592

Wang H, Smith HL, Kuang Y, Elser JJ (2007) Dynamics of stoichiometric bacteria-algae interactions in the epilimnion. SIAM J Appl Math 68(2):503–522

Wang WD, Zhao XQ (2012) Basic reproduction numbers for reaction–diffusion epidemic models. SIAM J Appl Dyn Syst 11(4):1652–1673

Wang Y, Shi JP, Wang JF (2019) Persistence and extinction of population in reaction-diffusion-advection model with strong Allee effect growth. J Math Biol 78(7):2093–2140

Yan YW, Zhang JM, Wang H (2022) Algae-bacteria interactions with nutrients and light: a reaction–diffusion–advection model. J Nonlinear Sci 32(4):1–36

Yoshiyama K, Mellard JP, Litchman E, Klausmeier CA (2009) Phytoplankton competition for nutrients and light in a stratified water column. Am Nat 174(2):190–203

Zhang JM, Kong JD, Shi JP, Wang H (2021) Phytoplankton competition for nutrients and light in a stratified lake: a mathematical model connecting epilimnion and hypolimnion. J Nonlinear Sci 31(2):1–42

Zhang JM, Shi JP, Chang XY (2018) A mathematical model of algae growth in a pelagic-benthic coupled shallow aquatic ecosystem. J Math Biol 76(5):1159–1193

Zhang JM, Shi JP, Chang XY (2021) A model of algal growth depending on nutrients and inorganic carbon in a poorly mixed water column. J Math Biol 83(2):1–30

Zhao XQ (2017) Dynamical systems in population biology, 2nd edn. CMS Books in Mathematics/Ouvrages de Mathématiques de la SMC. Springer, Cham